(2)

DTIC FILE COPY

DNA-TR-87-226-V2

CIVIC IMPROVEMENT PROGRAM

Volume II—Fallout Protection Factor Analysis Capability

J. A. Stoddard
Science Applications International Corporation
10260 Campus Point Drive
San Diego, CA 92121

15 August 1987

Technical Report

CONTRACT No. DNA 001-85-C-0375

Approved for public release;
distribution is unlimited.

THIS WORK WAS SPONSORED BY THE DEFENSE NUCLEAR AGENCY
UNDER RDT&E RMC CODE X3840854692 RN RA 00001 25904D.

Prepared for
Director
DEFENSE NUCLEAR AGENCY
Washington, DC 20305-1000

DISTRIBUTION LIST UPDATE

This mailer is provided to enable DNA to maintain current distribution lists for reports. We would appreciate your providing the requested information.

☐ Add the individual listed to your distribution list.

☐ Delete the cited organization/individual.

☐ Change of address.

NAME: _____

ORGANIZATION: _____

OLD ADDRESS	CURRENT ADDRESS
_____	_____
_____	_____
_____	_____
TELEPHONE NUMBER: ( ) _____	_____

SUBJECT AREA(s) OF INTEREST:

_____	_____
_____	_____
_____	_____

DNA OR OTHER GOVERNMENT CONTRACT NUMBER: _____

CERTIFICATION OF NEED-TO-KNOW BY GOVERNMENT SPONSOR (if other than DNA):

SPONSORING ORGANIZATION: _____

CONTRACTING OFFICER OR REPRESENTATIVE: _____

SIGNATURE: _____

CUT HERE AND RETURN

Director
Defense Nuclear Agency
ATTN: [redacted] TITL
Washington, DC 20305-1000

Director
Defense Nuclear Agency
ATTN: [redacted] TITL
Washington, DC 20305-1000

REPORT DOCUMENTATION PAGE

1a REPORT SECURITY CLASSIFICATION: UNCLASSIFIED	1b RESTRICTIVE MARKINGS:
2a SECURITY CLASSIFICATION AUTHORITY: N/A since Unclassified	3 DISTRIBUTION/AVAILABILITY OF REPORT: Approved for public release; distribution is unlimited.
2b DECLASSIFICATION/DOWNGRADING SCHEDULE: N/A since Unclassified	
4 PERFORMING ORGANIZATION REPORT NUMBER(S): SAIC-87/1746	5 MONITORING ORGANIZATION REPORT NUMBER(S): DNA-TR-87-226-V2
6a NAME OF PERFORMING ORGANIZATION: Science Applications International Corporation; 6b OFFICE SYMBOL (If applicable):	7a NAME OF MONITORING ORGANIZATION: Director, Defense Nuclear Agency
6c ADDRESS (City, State, and ZIP Code): 10260 Campus Point Drive, San Diego, CA 92121	7b ADDRESS (City, State, and ZIP Code): Washington, DC 20305
8a NAME OF FUNDING/SPONSORING ORGANIZATION; 8b OFFICE SYMBOL (If applicable): NANF/Moberley	9 PROCUREMENT INSTRUMENT IDENTIFICATION NUMBER: DNA 001-85-C-0375
8c ADDRESS (City, State, and ZIP Code):	10 SOURCE OF FUNDING NUMBERS: PROGRAM ELEMENT NO. 62715H; PROJECT NO. RN; TASK NO. RA; WORK UNIT ACCESSION NO. DH008948

11 TITLE (Include Security Classification)
CIVIC IMPROVEMENT PROGRAM
Volume II—Fallout Protection Factor Analysis Capability

12 PERSONAL AUTHOR(S)
Stoddard, J. A.

13a TYPE OF REPORT	13b TIME COVERED	14 DATE OF REPORT (Year, Month, Day)	15 PAGE COUNT
Technical	FROM 850915 TO 870815	870815	68

16 SUPPLEMENTARY NOTATION
This work was sponsored by the Defense Nuclear Agency under RDT&E RMC Code X3840854692 RN RA 00001 25904D.

17 COSATI CODES		
FIELD	GROUP	SUB-GROUP
12	5	
24	6	

18 SUBJECT TERMS (Continue on reverse of necessary and identify by block number)
Fallout, CIVIC, Casualty Assessment, Protection Factors, Radiation Transport, Civil Defense, Vehicle Code System, SNA

19 ABSTRACT (Continue on reverse if necessary and identify by block number)

The Vehicle Code System (VCS), originally developed to calculate initial radiation environments and protection factors for three-dimensional shield systems, has been modified to calculate protection factors for fallout radiation environments. This report describes the modifications to VCS and gives the results of several test case analyses performed to verify this fallout protection factor version.

Fallout radiation protection factor calculations were performed for a number of structures for which simulated fallout experiments had been performed in the late 1950's and early 1960's. The comparisons were generally good, with about half of the results agreeing within 10 percent and three-quarters of the results agreeing

20 DISTRIBUTION/AVAILABILITY OF ABSTRACT	21 ABSTRACT SECURITY CLASSIFICATION	
☐ UNCLASSIFIED/UNLIMITED ☒ SAME AS RPT ☐ DTIC USERS	UNCLASSIFIED	
22a NAME OF RESPONSIBLE INDIVIDUAL: Sandra E. Young	22b TELEPHONE (Include Area Code): (202) 325-7042	22c OFFICE SYMBOL: DNA/OSTI

DD FORM 1473, 84 MAR — 83 APR edition may be used until exhausted. All other editions are obsolete.

19. ABSTRACT (Continued)

within 20 percent. Disagreement was found in some cases where descriptions of the structure were not adequate. We believe, based on these overall results, that the fallout protection factor version of VCS is performing correctly.

Calculations were also performed to assess the potential effect on fallout protection factors of a number of variations in typical structures. Variations explored included the effects of internal partitions, attached garages, basement depth, structure length-to-width ratio, and fallout contaminated balconies.

PREFACE

I wish to acknowledge the support of several people whose help resulted in the successful completion of this project. These include Dr. Paul Castleberry and LTC Joe Sims of Hq. DNA, whose patient support made this effort possible; Bill Scott and Mike Gritzner of SAIC, whose detailed knowledge of the original VCS computer program was instrumental to the development of the FPF version of VCS; Charles Eisenhauer of the National Bureau of Standards who provided encouragement and data from a number of fallout simulation experiments; Larry Gabriel of DNA Field Command and Chuck Caldwell of Holms and Narver, Inc., both at the Nevada Test Site, who facilitated our site visit to the NTS wood rambler and two-story brick test structures; Murray Schmoke of the Ballistic Research Laboratory, who aided in the description of the NDL concrete blockhouse; Bill Stockinger at Ft. Independence, Boston Harbor, and Paul White of the National Archives in Waltham, who, among others, helped search for information on the Long Island Barracks; and to Joe Manukas at the Long Island Hospital, who facilitated the visit to the remains of the Long Island Barracks.

TABLE OF CONTENTS

LIST OF ILLUSTRATIONS

LIST OF TABLES

SECTION 1
INTRODUCTION

1.1 GENERAL.

Three of the Civilian Vulnerability Indicator Code (CIVIC) improvement program tasks performed by SAIC were related to the development of fallout protection factors for use in CIVIC and other casualty assessment codes. These three fallout protection factor tasks are the following:

Task 7: Develop fallout protection factor distributions for the Soviet Union.

Task 8: Verify the fallout protection factor version of the VCS code by comparing the results of VCS calculations with the results of experiments.

Task 9: Calculate fallout protection factor variations for some typical structure categories.

The results of Tasks 7, which are classified, are given in volume 3 of this final report. The results of Tasks 8 and 9 are given below.

1.2 VERIFICATION OF THE FPFVCS.

In the 1950's and 1960's, before the availability of the current generation of large, high-speed computers, a significant effort was made by the Office of Civil Defense, the National Bureau of Standards and others to define the protection afforded by structures against fallout radiation from nuclear weapons. A major result of this effort was the "Engineering Method" for calculating fallout protection factors for structures, developed largely by the National Bureau of Standards (Refs. 1,2,3). The Engineering Method was derived semiempirically from gamma-ray attenuation calculations

of slabs and other relatively simple configurations and from experimental measurements of a number of test structures. The Engineering Method has been, and continues to be, used to calculate fallout protection factors for structures, for example by the Federal Emergency Management Agency for entries in the National Facility Survey (Ref. 4).

While the Engineering Method is based on a considerable amount of calculated and measured data, it is limited in application by its semiempirical nature to conditions for which it has been tested. It is very difficult to derive an empirical model which will adequately treat interactive scattering and streaming from walls, openings and other features common to complex three-dimensional structures.

With the development of large, high-speed computers it became possible to eliminate the limitations associated with the Engineering Method and to improve accuracy by the use of computer programs which are based on more fundamental physics. In the early 1970's, Cohen and Beer performed Monte Carlo transport calculations of a number of structures using the forward Monte Carlo SAM-CE code (Ref. 5). More recently, the Vehicle Code System (VCS) (Refs. 6,7) has been used to calculate initial radiation protection factors for Japanese structures for the dosimetry reassessment of Hiroshima and Nagasaki A-Bomb survivors (Ref. 8). For the latter effort, excellent agreement was obtained for VCS validation calculations of several Japanese-type structures tested in the Bare Reactor Experiment Nevada (BREN) test series (Ref. 9).

Several modifications to VCS were necessary to compute fallout protection factors. This report briefly describes these modifications and the results of verification calculations performed to date.

In all of the test cases used for verification, no new experimental data were derived; instead calculations were performed on experiments described in available literature. Most of these experiments were performed during the 1950's or early 1960's to calibrate the Engineering

Method. This caused some problems for the verification calculations because existing descriptions of the structures were not always been complete or accurate. This was especially a problem for the Long Island Barracks, which was demolished shortly after the experiments, and for which no as-built drawings have been found.

1.3 FPF VARIATIONS IN STRUCTURE CATEGORY.

In an effort conducted by SAIC for DNA in 1983-1984, fallout protection factors were calculated for a matrix of 64 U. S. residential structure categories, including 34 categories of single family structures and 30 categories of multiple family structures. In that work, in which fallout protection factor distributions were derived for the U.S., generally only one fallout protection factor calculation was performed per structure category, and the result of that one protection factor calculation was assumed to represent all structures in the category.

In Task 9 of this CIVIC improvement effort a number of FPFVCS calculations were performed to investigate the variation of protection factors within a typical structure category. Protection factor variations within a given structure were also explored by calculating the protection factor at different locations within the structure.

Three structures were analyzed, a one-story wood frame house, a two-story brick faced house and a four-story brick faced apartment house. Basements were modeled for all three structures so that protection factors of shelter locations both in the basement and on above-ground floors could be evaluated.

A similar approach to the analysis of the three structure types was adopted. First a baseline structure was defined. Protection factor traverses in the basement and on above-ground floors were performed. Then variations in the structure were modeled and analyzed.

1.4 ORGANIZATION OF THIS VOLUME.

This volume is divided into six sections. Following this introduction (Section 1) is a short summary and conclusions (Section 2). Section 3 gives a brief description of the Vehicle Code System and data used, Section 4 presents the results of validation calculations, Section 5 describes the calculations of protection factor variations, and Section 6 lists the references.

SECTION 2
SUMMARY AND CONCLUSIONS

2.1 VCS CODE MODIFICATION AND VERIFICATION.

This report briefly describes the changes made to the adjoint Monte Carlo Vehicle Code System (VCS) to compute fallout radiation protection factors for complex three-dimensional structures. The primary modifications made to VCS to permit the treatment of fallout radiation sources are (1) the addition of logic to score particles at potential source surfaces (e.g., roof and ground surfaces) within the Monte Carlo geometry, (2) the addition of logic in the coupling code to treat these new scores, (3) the addition of a capability to couple with ANISN plane geometry free-field fluxes instead of the two-dimensional DOT free-field fluxes, and (4) the development of a fallout source spectrum in an energy group format consistent with an available gamma-ray cross section set.

Several test calculations have been performed for comparison with available experimental data to verify the correct operation of the code. Test cases discussed here include (1) calculation of the dose rate at a height of 3 feet above an infinite Cobalt 60 contaminated plane, (2) comparison of the uncollided portion of the dose at a distance of 3 feet from disk sources of various sizes, (3) calculation of the protection factor for a foxhole, (4) calculation of the dose rates within a concrete blockhouse, (5) calculation of dose reduction factors (inverse protection factor) for a wood frame house with basement, (Kansas State University house), (6) calculation of dose rates in a wood frame house on a slab, (7) calculation of dose rates in a two-story brick house with basement, and (8) calculation of dose rates in a large three-story brick structure, the Long Island (Boston Harbor) Barracks.

With some notable exceptions, the comparisons were generally good, with about half of the results agreeing within 10 percent and three-quarters of the results agreeing within 20 percent. The major exceptions were

some of the Kansas State University house comparisons and some of the Long Island Barracks comparisons. It is expected that these major discrepancies, which sometimes involved dose rate differences by a factor of two or more, are the result of an incomplete or inadequate description of the structure geometry and materials.

It has been our experience that comparisons between VCS calculations and experimental results generally improve with better descriptions of the structure. In this effort, significant differences between VCS calculated and measured dose rates for the Nevada Test Site two-story brick structure were observed until on-site measurements were made which indicated a 22 lb/ft^2 discrepancy between the reported and actual mass wall thickness. Significant improvement in the comparisons of calculated and measured dose rates for the Long Island Barracks was also seen when on-site measurements of still standing parts of the exterior walls showed a similar 20 lb/ft^2 discrepancy for that structure. Similarly, in a previous effort in which we used VCS to calculate initial radiation protection factors for Japanese-type structures for the Bare Reactor Experment Nevada (BREN) tests (Ref. 9), discrepancies remained between calculated and measured results until a site visit revealed errors in the definition of the test structures.

It is our opinion that the fallout version of VCS is performing correctly, and that differences between calculated and measured results are, except for Monte Carlo statistics, caused by inadequacies in the geometry and materials model arising from inaccurate or inadequate descriptions of the structures. It is also our opinion that, overall, especially taking into account the structures for which the geometry was well defined, the results of these comparisons indicate that the code system is giving good results.

2.2 FPF VARIATIONS IN STRUCTURE CATEGORY.

The variation in protection factors for variations of structures within a structure category were analyzed for three structure types: a wood frame house with basement, a two-story brick face house with basement, and a three-to five-story brick face apartment building with basement. For all three cases a baseline structure was defined, protection factor traverses of the structure were made, and the effects of excursions on the baseline were explored.

Protection factor variations with location within a structure was, as expected, most pronounced for basement vs non-basement locations. This effect was known and basement vs non-basement locations had been carefully treated in the U.S. protection factor study conducted by SAIC in 1983-1984. Of more interest here is the variation of protection factors with location in the basement or with location changes on above-ground floors. For the single-family houses, protection factors varied by about 30 percent with basement location, with the highest protection factors being in corner locations. At above-ground locations, protection factors varied by about 15 percent with the largest protection factors being near the center of the house. Very little difference between protection factors on the first floor and the second floor were seen for the two-story brick face house.

The protection factor variation with location in the apartment building was larger, with factor-of-two variations seen for similar locations on different floors. The protection factors on intermediate floors were larger than the protection factors for the first and top floors.

The effects of several structure variations were explored. Addition of an attached garage to the single-story wood frame house decreased the protection factor in the basement by about 5 percent and had an insignificant effect on the protection factors on the first floor. Varying the basement depth from 50 to 80 inches in the same structure

changed the protection factors by about 35 percent. Change of the two story brick house length to width ratio from 1.14 to 1.56, while maintaining the same foor area, produced a negligible effect on the protection factor at the center of the house. However doubling the window sizes (by window area) in that structure decreased the protection factor by about 30 percent. Addition of fallout contaminated balconies to the apartment house resulted in a negligible change in the protection factor at the center of that structure.

The effect of partitions (interior walls) was investigated in all three structures by performing calculations both with and without the partitions. The effect of partitions was found to be significant for the single story wood frame house (20 percent), where the partitions represented a significant portion of the material mass between the protection factor location and the building exterior. The mass of the interior partitions was not so large compared to the mass thickness of the walls of the two story brick house, and the partitions affected the protection factor by only about 10 percent in that structure. In the apartment house, however, where there were many partitions and where the windows were large, the partitions had nearly a factor of two effect on the protection factor.

Overall, while some variations in the protection factor with variations in the structure were observed, no major effects were seen that would be expected to change the results of the U. S. fallout protection factor distribution study performed by SAIC in 1983-1984. Instead, the results found here tend to indicate that the categorizations used in that study adequately describe the protection afforded by residences in the U.S.

SECTION 3
DESCRIPTION OF THE FALLOUT PROTECTION FACTOR VERSION OF VCS

3.1 DESCRIPTION OF THE ORIGINAL VCS.

The Vehicle Code System was derived primarily to calculate initial radiation environments in armored vehicles from nuclear weapons bursts. To facilitate the solution of this 3-dimensional deep penetration problem, the VCS divides the calculation into two parts: a 3-D adjoint Monte Carlo analysis of the armored vehicle, and a 2-D discrete ordinates calculation of the free-field environment. In VCS, the 3-D adjoint Monte Carlo analysis is performed with the MORSE computer code (Ref. 10), and the 2-D discrete ordinates free-field calculation is performed with DOT (Ref. 11). A third code, DRC, is used to couple the adjoint fluxes from MORSE with the free-field environments from DOT to calculate radiation environments or protection factors at "detector" locations in the vehicle or structure.

This analysis procedure is illustrated in Figure 1, which shows an armored vehicle in the vicinity of a nuclear weapon burst. The armored vehicle is enclosed in a "Monte Carlo problem boundary". The transport of radiation in the vehicle, air and soil within this boundary is calculated by adjoint Monte Carlo, and the adjoint flux results are coupled with the free-field fluxes at the Monte Carlo problem boundary.

The theory for the above adjoint/free-field coupling methodology is discussed in the literature, for example, Hoffman, et al. (Ref. 12). The method permits the radiation transport analyses of complicated three-dimensional structures without the requirement to perform the expensive deep penetration analyses of free-field air transport in the atmosphere exterior to the vehicle. The theory for the treatment of adjoint particles is solidly based on the mathematics of the linear Boltzmann transport equation, as described by Ref. 13, the only approximation being that the vehicle must not significantly perturb the inward directed portion of the free-field environment. This latter condition is met by including the soil

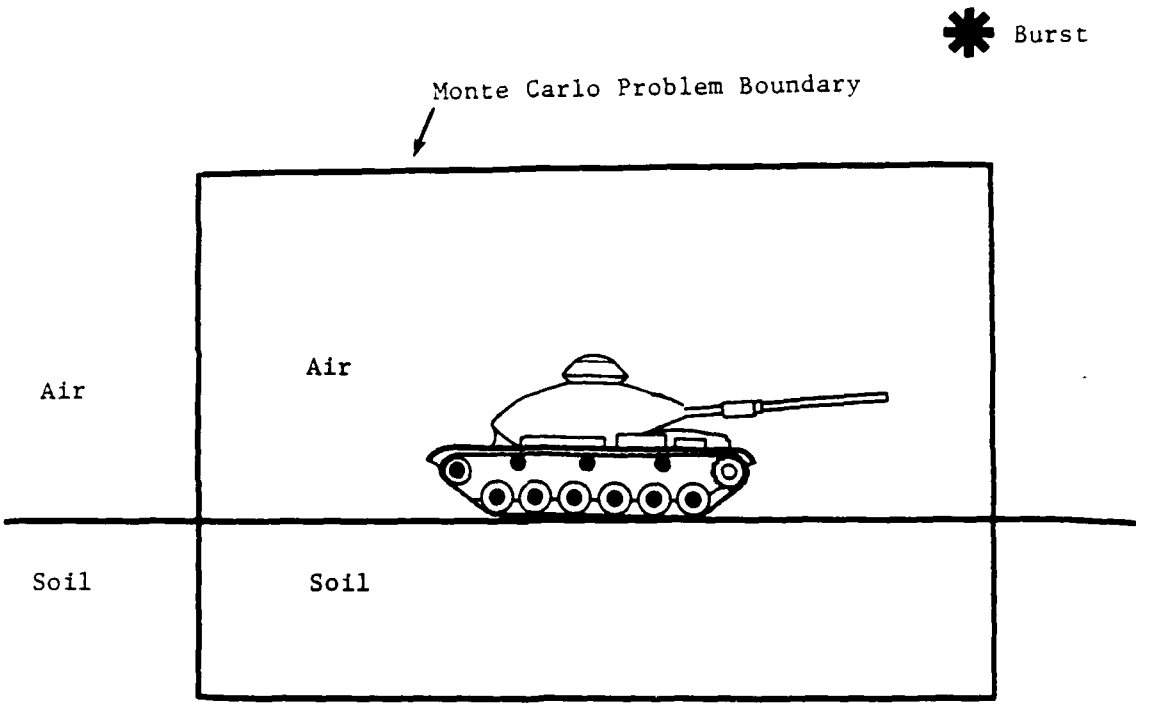

Figure 1. VCS analysis geometry for initial radiation.

in the Monte Carlo geometry and may be further assured by placing the Monte Carlo boundary surface at a reasonable distance from the vehicle. For the fallout protection factor analyses discussed later in this report, this boundary was taken to be several hundred meters from the structure. This not only assured that the structure would not perturb the free-field environment; it allowed the analysis of large or multiple structures without the need to readjust the coupling parameters in the DRC code.

The Monte Carlo analysis of the adjoint flux in the three-dimensional geometry involves following the radiation particles backwards along their flight path from the radiation "detector" location (D in Fig. 1) to the "escape" from the Monte Carlo problem boundary. This following of particles backwards in flight, besides being equivalent to the theoretical adjoint treatment, has the physical advantage for Monte Carlo of starting particles at a point and scoring on large surfaces. This is very helpful for obtaining good statistics in Monte Carlo analyses because (1) fewer particle flights are needed to describe a point particle source than a large source, and (2) more scores are generated when the scoring surface is large and therefore easier to "hit" in Monte Carlo random walks, thereby improving the statistics of the calculations.

3.2 MODIFICATIONS TO CALCULATE FALLOUT PROTECTION FACTORS.

For the calculation of fallout protection factors, it was necessary to make several modifications to VCS. These changes included the addition of logic in MORSE to score particles which intersect fallout bearing surfaces within the Monte Carlo geometry (Figure 2) and the modification of DRC to treat these scores. Also, since the free-field radiation environment is well characterized by a one-dimensional discrete ordinates calculation in plane geometry, DRC was modified to couple to ANISN (Ref. 14) free-field fluxes instead of the two-dimensional DOT free-field fluxes. These changes are described below, after a brief description of the way that VCS calculates fallout protection factors.

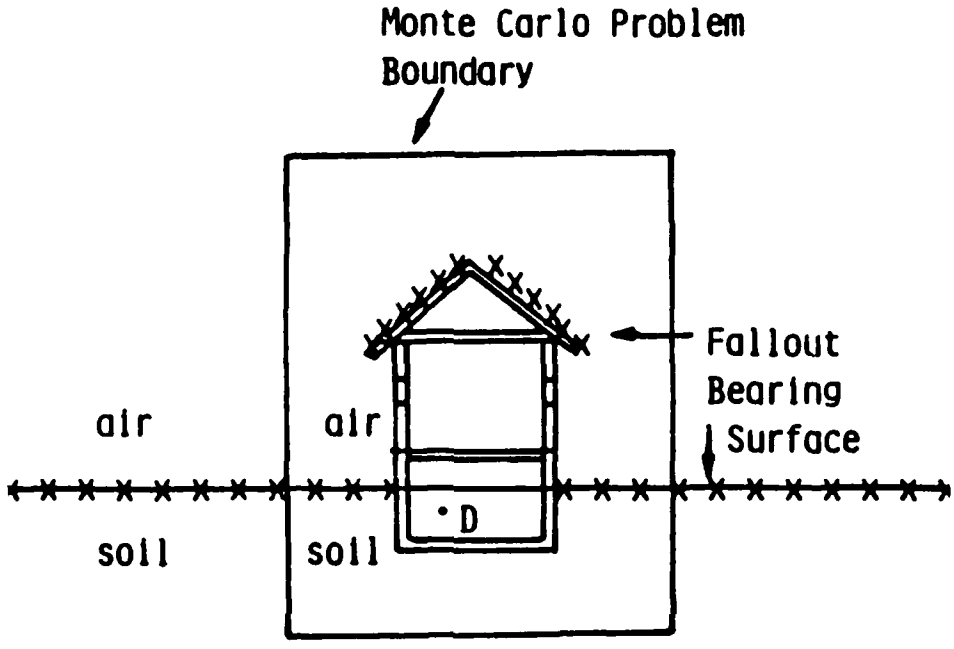

Figure 2. VCS analysis geometry for fallout.

The calculation of fallout protection factors using VCS proceeds as follows. First, the energy- and angle-dependent gamma ray free-field environment from radioactive fallout is calculated with the one-dimensional ANISN discrete-ordinates code using an infinite plane fallout spectrum source on the soil surface. This calculation needs to be performed only once since the resulting energy-, angle-, and elevation-dependent flux data can be used for as many protection factor calculations as desired. The geometry and material cross sections for the structure in question are then prepared for input to the MORSE part of VCS. As with VCS calculations of initial radiation, this geometry is defined, including the soil surface, out to a "Monte Carlo Problem Boundary" surface. In the MORSE calculation, adjoint particles are started at the detector location (D in Figure 2) and followed backwards until they reach the Monte Carlo problem boundary surface. A computer file of adjoint particle scores is created, with scores made for each adjoint particle crossing of a fallout bearing surface (generally the soil surface and all roofs within the Monte Carlo geometry) and each crossing of the Monte Carlo boundary surface (a particle "escape").

After completion of the MORSE calculation, the MORSE output file of particle scores is coupled with the free-field flux from ANISN via the DRC code.

As mentioned, the fallout protection factor version of DRC treats two types of scores from MORSE: scores for particles crossing fallout contaminated surfaces (generally roofs and soil surfaces within the Monte Carlo problem boundary), and particles which "escape" the Monte Carlo problem boundary. With the two types of scores recorded by MORSE, it was necessary to label each score as coming from an "escape" event or from a "boundary crossing" at a fallout bearing surface. DRC then evaluates the dose at the detector with the following expression, the second term of which was added to treat the boundary crossing scores:

$$\text{Dose} = \frac{1}{\text{NHIST}} \left[\sum_{\substack{\text{Escape} \\ \text{Scores}}} \frac{\psi_m(\text{IG},\text{H}) \cdot \text{WATE}(\underline{\Omega},\text{IG},\text{IGS},\text{H}) \cdot \text{R}(\text{IGS})}{\text{R}^*(\text{IGS})} + \sum_{\substack{\text{Boundary} \\ \text{Crossing} \\ \text{Scores}}} \frac{\text{S}(\text{IG}) \cdot \text{WATE}(\underline{\Omega},\text{IG},\text{IGS},\text{H}) \cdot \text{R}(\text{IGS}) \cdot \cos\theta}{(\underline{\Omega} \cdot \underline{n}) \cdot \text{R}^*(\text{IGS})} \right]$$

In the above,

NHIST is the number of particle histories simulated with MORSE,

$\psi_m(\text{IG},\text{H})$ is the angle-, energy group- and elevation-dependent angular free-field radiation flux from ANISN,

$\text{WATE}(\underline{\Omega},\text{IG},\text{IGS},\text{H})$ is the weight of a scoring particle (boundary crossing or escape) of angle $\underline{\Omega}$, energy group IG, starting energy group IGS, and elevation H,

R(IGS) is the detector response function for the energy group of the adjoint source particle at the detector,

$\text{R}^*(\text{IGS})$ is the source bias function used in MORSE,

S(IG) is the source strength for the energy group of the particle at the scoring surface,

$\underline{\Omega} \cdot \underline{n}$ is the cosine of the angle formed by the particle unit vector, $\underline{\Omega}$, and the normal to the scoring surface, $\underline{n}$, and

$\cos\theta$ is the cosine of the roof or ground slope at the scoring location. This factor is used to maintain a constant source strength per unit of horizontally projected roof or soil area.

The ease of scoring for adjoint Monte Carlo particles is affected not only by problem geometry but by source and response function energy considerations. In "following" adjoint particles backwards starting at the "adjoint source" at the detector, the energy of the starting adjoint particle is selected randomly from the response function (e.g., tissue kerma), and scoring is weighted by the energy spectrum of the fallout source. Since

the fallout source spectrum is broad, non-zero contributions are made for most Monte Carlo scores. However, for calculations of fallout protection factor experiments which used Cobalt 60 as the simulated fallout source, many Monte Carlo scores resulted in zero contributions because of the discrete Cobalt 60 gamma-ray energy emissions. This, plus the fact that experiments can simulate only finite sized (rather than infinite plane) sources makes the verification calculations of experimental results much more difficult than production calculations of fallout protection factors.

To improve the statistics of VCS analyses where ring sources or narrow annular area sources of Co-60 were used, a set of additional logic has been added to MORSE to improve statistics. This logic, which is based on the standard MORSE next-event estimation technique, provides a particle score at a randomly selected point on the ring each time that a scattering event occurs in the Monte Carlo geometry. The score made is the following:

$$\text{Score} = \frac{W\, P(\mu)\, e^{-\eta}}{R^2}$$

where W is the particle weight before the scattering event, $P(\mu)$ is the probability that the particle will scatter through angle of cosine μ toward the randomly selected point on the ring [$P(\mu)$ is calculated from cross section data by an available subroutine in VCS], η is the number of mean free paths, and R is the distance from the scattering point to the scoring point on the ring.

The 36 group cross section set, DLC-48/PVC, was used for the calculations. This cross section set is the gamma only part of the 207 group DLC-VITAMIN-C neutron plus gamma cross section set (Ref. 15). Table 1 lists the energy grouping for the 36 group cross section set along with the Cobalt 60 source spectrum, the fallout source spectrum and the tissue response kerma used in the fallout and validation calculations. The Cobalt 60 source spectrum is simple, containing a 1.0 for a source of one disintegration per second per square centimeter of source area for each of the two

Table 1. Thirty-six group fallout source spectrum and tissue response function.

Energy Group	Energy Band (Mev)	Co-60 Source Spectrum	Fallout Source Spectrum	Tissue Response Kerma
1	12.000-14.000	0	0	3.250E-09
2	10.000-12.000	0	0	2.830E-09
3	8.000-10.000	0	0	2.419E-09
4	7.500-8.000	0	0	2.143E-09
5	7.000-7.500	0	0	2.038E-09
6	6.500-7.000	0	0	1.932E-09
7	6.000-6.500	0	0	1.827E-09
8	5.500-6.000	0	1.964E-08	1.723E-09
9	5.000-5.500	0	3.922E-08	1.617E-09
10	4.500-5.000	0	1.069E-09	1.513E-09
11	4.000-4.500	0	7.349E-05	1.403E-09
12	3.500-4.000	0	5.345E-04	1.288E-09
13	3.000-3.500	0	4.593E-03	1.170E-09
14	2.500-3.000	0	1.851E-02	1.050E-09
15	2.000-2.500	0	4.987E-02	9.150E-10
16	1.660-2.000	0	3.574E-02	7.915E-10
17	1.500-1.660	1	5.077E-02	7.102E-10
18	1.330-1.500	1	6.480E-02	6.541E-10
19	1.000-1.330	0	1.062E-01	5.636E-10
20	0.800-1.000	0	1.964E-01	4.562E-10
21	0.700-0.800	0	1.009E-01	3.884E-10
22	0.600-0.700	0	9.620E-02	3.407E-10
23	0.512-0.600	0	7.082E-02	2.948E-10
24	0.510-0.512	0	1.537E-03	2.708E-10
25	0.405-0.510	0	4.743E-02	2.542E-10
26	0.400-0.450	0	4.189E-02	2.248E-10
27	0.300-0.400	0	1.002E-01	1.835E-10
28	0.200-0.300	0	5.959E-02	1.255E-10
29	0.150-0.200	0	4.475E-02	8.330E-11
30	0.100-0.150	0	3.808E-02	5.560E-11
31	0.075-0.100	0	1.136E-02	4.116E-11
32	0.060-0.075	0	6.013E-03	4.065E-11
33	0.045-0.060	0	6.681E-03	4.902E-11
34	0.030-0.045	0	8.017E-03	7.340E-11
35	0.020-0.030	0	6.681E-03	1.603E-10
36	0.010-0.020	0	8.084E-03	5.220E-10

Cobalt 60 discrete emission energies (1.17 and 1.33 MeV). The fallout source spectrum is based on data from Ref. 16 for gamma rays one hour after U-235 fission, and the tissue kerma response function was derived from the 21 gamma group DLC-31 set (Ref. 17).

Cross sections were mixed for standard densities of air and soil plus a number of common construction materials, including wood, concrete, plaster, etc. The elemental compositions and the density of the mixed results are given in Table 2. In the MORSE calculations, it was necessary to further mix these materials to obtain cross sections for major structure elements such as "external wall", "foundation", floor and ceiling", "internal partitions," etc. This operation was performed in MORSE by entering the various materials comprising the structure element along with the volume percent of the component. For example, a 4.5-inch thick internal partition might be comprised of a 0.5 inch plasterboard layer on each side supported by 1.5-in x 3.5-in two-by-four studding on 16-inch centers. The volume fractions for these components would be 0.222 (1/4.5) for the plasterboard and 0.073 (1.5 x 3.5/ 4.5 x 16) for the wood. When density information is available for the components of specific structures, adjustments are made by multiplying the volume fraction of that component by the ratio of the measured density to the density for the reference material.

Table 2. Material compositions for cross sections (numbers are percent by weight).

Composition	Air	Soil	Wood	Concrete	Common Brick	Fire Clay Brick	Mortar	Stucco	Plaster	Asphalt Shingle	Clay Tile
Density (g/cm^3)	0.00101	1.7	0.51	2.24	1.92	2.08	1.86	1.86	0.80	1.12	2.31
H-1	---	1.3	6.3	0.6			0.7	1.3	1.1	1.0	1.2
C-6	---	0.9	49.2						1.3	30.0	
N-1	75.5	0.01									
O-8	23.2	50.4	44.5	49.8	52.5	49.7	46.0	53.5	66.6	29.2	44.7
Na-11	---	0.7		1.7			2.0	0.4			
Mg-12	---	2.1		0.2		0.6	3.7	0.2			
Al-13	---	9.1		4.5	0.5	21.2	5.9	0.4			16.0
Si-14	---	25.9		31.7	44.9	25.2	21.2	33.5		3.6	33.2
P-15	---	0.02									
S-16	---	0.03		0.1				0.07	8.3		
Ar-18	1.3										
K-19	---	2.0		1.9				0.04			
Ca-20	---	6.9		8.3	1.4	0.7	12.8	10.6	20.9	36.2	
Ti-22	---					1.2					
Mn-25	---	0.08									
Fe-26	---	0.6		1.2	0.7	1.4	7.7	0.4			4.9

SECTION 4
RESULTS OF VALIDATION CALCULATIONS

This section describes the results of comparisons between calculations made with the fallout protection factor version of VCS and experimental data or accepted calculated results. The following test cases are analyzed: dose rate 3 feet above an infinite Cobalt 60 plane source (Section 4.1), analytic solution of uncollided dose from a disk source (Section 4.2), foxhole (Section 4.3), NDL blockhouse (Section 4.4), KSU house (Section 4.5), wood frame house (Section 4.6), two-story brick house (Section 4.7), and Long Island (Boston Harbor) Barracks (Section 4.8).

4.1 COBALT 60 INFINITE PLANE SOURCE.

The first case was the dose rate at a height of 3 feet above an infinite plane contaminated with 1 curie/ft^2 of Cobalt 60. Several different estimates of this dose rate are reported in the literature. For example, Spencer (Ref. 2) lists experimental results by Rexroad and Schmoke, (497 R/hr), McDonnel, et al., (464 R/hr) and Schumchyk, et al., (468 R/hr), and calculates a value of 482 R/hr. Eisenhauer (Ref. 18) calculated a value of 500 R/hr, and MAGI (Ref. 5) calculated a value of 492 R/hr.

A value of 493 R/hr was calculated with VCS and air and soil cross sections based on the compositions shown in Table 2. This value is within a few percent of all the above estimates.

4.2 ANALYTIC RESULTS FOR A DISK SOURCE.

Based on integration of radiation doses from a point isotropic source, Foderaro (Ref. 19) gives the uncollided dose rate for a shielded disk source:

$$\dot{D}_u = \frac{K(E)\ ES_a}{2} [E_1\ (b_1) - E\ \ (b_1 \sec \theta)]$$

where $\dot{D}_u$ is the dose rate from uncollided photons (R/hr),

$K(E)$ is an energy flux to dose rate conversion factor (R/hr per MeV/cm^2-sec)

E is energy of source photon (MeV)

S_a is source strength per unit area (cm^{-2} sec^{-1}),

E_1 is an exponential integral function (dimensionless),

b_1 is shield optical thickness (dimensionless), and

θ is angle subtended by a disk radius as viewed from the detector.

Uncollided dose rates from ten disk sources ranging from 10 cm radius to 100 meter radius were calculated from the above expression and with VCS. Comparison of the results was excellent, with seven of ten values agreeing within two percent and all but one agreeing within four percent. The largest difference was 8.8 percent, for the 10-cm disk source, which suffered from statistics as indicated by a VCS fractional standard deviation of 9 percent for that calculation.

4.3 FOXHOLE.

Reference 2 describes experimental and calculated exposure factors for foxholes of various geometries. The primary source of fallout radiation dose in an uncontaminated foxhole is "skyshine" from photons scattered in the atmosphere. A secondary source of dose in the foxhole is radiation from sources at or near the foxhole lip which is transmitted through the soil.

Based on the data in Ref. 2 (pp. 428-442), a protection factor of 100 was derived for a foxhole with a solid angle view of the sky of 0.3 steradians. This protection factor included radiation from both skyshine and the foxhle lip. A 5 ft by 5 ft (square cross section) foxhole 8.8 ft deep with the detector point at a depth of 5.8 ft below the soil surface was modeled for the VCS calculation. The VCS result for this foxhole was a protection factor of 93.5, which differed from the Ref. 2 value by about 7 percent.

4.4 NDL BLOCKHOUSE.

References 2 and 20 also describe the results of dose reduction factor measurements made in 1957 on a concrete blockhouse at the Nuclear Defense Laboratory (now part of the Ballistic Research Laboratory). The basic blockhouse is described as a square structure 12 ft on a side and 8 ft high of 4-inch poured concrete for a wall thickness of about 47 lb/ft^2. The blockhouse contained 2 ft x 2 ft windows centered in three of the four walls, but these were filled with concrete blocks. The fourth wall had a 2 ft by 6 ft doorway with a 47 lb/ft^2 sliding door. Except for a 1 ft cubical hole dug in the center of the floor, it was essentially an above grade structure. The roof of the basic blockhouse was comprised of 0.5 inch plywood and 1 1/32 inch steel supported by a standard 10 inch wide-flange I beam.

Separate dose measurements were made for roof and for ground sources. Fallout on the roof was simulated by a grid of point Cobalt 60 sources spaced at 2 feet intervals, and the ground sources were simulated by a grid of point Cobalt 60 source on the ground. For both roof and ground sources, symmetry of the structure and detector locations was used to reduce the number of cobalt sources required by a factor of eight. On the ground, a variable grid spacing was also used, with a higher density of sources placed near the blockhouse. Sources were placed out to a distance of 405 ft from the blockhouse.

Dose measurements were made for several roof and wall thicknesses and for several detector elevations above the center of the floor. For comparison with VCS calculations, 48 lb/ft^2 data for the basic blockhouse roof and wall thicknesses of 42.17 lb.ft^2 and 48 lb/ft^2 respectively, were selected.

The experimentally measured and calculated doses are compared in Table 3 below. All of the results agree within 10 percent.

Table 3. Comparison of results for the NDL blockhouse.
(Doses in R/hr per curie/ft^2 source)

Source	Experiment	VCS	Ratio
Roof	22.7	23.1	0.98
Ground to 84.4 ft	88.9	98.3	0.90
Ground to 405 ft	128	131.6	0.97

4.5 KSU HOUSE.

The Kansas State University house (Ref. 21) was a 30 ft x 40 ft structure constructed for the purpose of making protection factor measurements on "typical American" houses. It had special design features which allowed the variation of the exterior wall thickness, internal partition configuration and exposed basement wall height and thickness. The above variability was achieved by stacking concrete blocks or panels around the exterior wall to alter the wall thickness from 5.5 lb/ft^2 to 45.5 lb/ft^2, by moving the internal partitions, and by raising or lowering the floor, which was supported by jack posts. It also had a 9 feet deep basement.

Fallout on the ground was simulated by the use of Cobalt 60 sources in a hydraulic source circulation system. Taking into account the symmetry of the test structure, source tubing was placed in three zones. Zone 1 extended from the exterior wall of the house to a radius of 80 ft

from the center of the house. Zone 1 had a 12 inch spacing between source tubes. Zone 2 extended from the edge of Zone 1 to a radius of 125 ft from the center of the house. Zone 2 used a 18 inch tube spacing. Last, Zone 3 extended from Zone 2 to a distance of 169 ft from the house center, and used a 24 inch tube spacing. No sources were placed on the roof.

VCS comparison calculations were performed for three detector/ structure configurations: A detector 3 ft cm above the center of the first floor for the structure with 5.5 lb/ft^2 exterior walls, detector 3 ft above the center of the basement floor for the structure with 5.5 lb/ft^2 exterior walls, and detector 3 ft above the center of the basement floor for the structure with 45.5 lb/ft^2 exterior walls. The dose reduction factor results (reciprocal of protection factor), given by source ring, are given in Table 4.

Table 4. Comparison of VCS with experiment for Kansas State University house.

Wall Thickness $(lb/ft)^2$	Detector Location	Source Ring	Expt.	VCS	Ratio
5.5	First Floor	1	0.178	0.237	0.75
		2	0.046	0.072	0.64
		3	0.028	0.030	0.93
5.5	Basement	1	0.0056	0.0113	0.49
		2	0.0020	0.0015	1.33
		3	0.0012	0.0011	1.11
45.5	Basement	1	0.0070	0.0056	1.23
		2	0.0021	0.0020	1.03
		3	0.0013	0.0013	1.02

Agreement between measured and calculated values for the KSU house is not consistent, with differences ranging from 2 percent to a factor of two. The high values of the VCS dose reduction factors for the first floor detector suggest that the actual mass thickness of the exterior wall was larger than the 5.5 lb/ft^2 indicated. The radiation dose for a first or second story detector in a thin-walled structure with no roof source is generally dominated by uncollided radiation transmitted through the walls, doors and windows directly from the source. A mass wall thickness greater

than the 5.5 lb/ft^2 would have caused more attenuation of the direct radiation, thus resulting in smaller measured dose reduction factors than calculated with VCS.

The dose contribution to basement detectors in a structure with no roof source is, however, more complicated. Except for a small amount of radiation transmitted through the lip of the basement wall, the uncollided dose from soil sources is almost totally eliminated by attenuation in the soil. If the structure has thin walls, ceilings and roofs, skyshine (gammas scattered in the atmosphere) is usually the dominant dose contributor. If the structure has thicker walls, ceilings and roofs, the contribution by skyshine is decreased by attenuation while the contribution from gammas scattered by above-ground components of the structure is increased.

For thin structures with no roof source, the net effect in an increase in the mass thickness of the exterior wall can be to increase the dose at a basement detector. As shown in Figure 4-4 of Ref. 21, an increase in the dose at the basement detector is expected with an increase in the 5.5 lb/ft^2 KSU house exterior wall thickness. Thus the basement detector reading for source ring 2 (ratio of 1.33 in Table 4) appears to be consistent with the postulate that the wall thickness is greater than 5.5 lb/ft^2. This does not, however, explain the basement detector reading for source ring 1 (ratio of 0.49 in Table 4). The inconsistencies between the measured and calculated dose reduction factors for the KSU house, therefore, remain unexplained.

4.6 NTS WOOD RAMBLER.

The NTS wood rambler is one of several residential type structures built at the Nevada Test Site for the 1953 test series. As described in Refs. 18 and 22, the wood rambler is a single-story wood frame structure built on a slab. Its outside dimensions were 40 ft by 25 ft 4 inches. Figure 3 shows computer drawn front and rear views of the structure. Reference 18 describes the wood rambler as being of conventional design

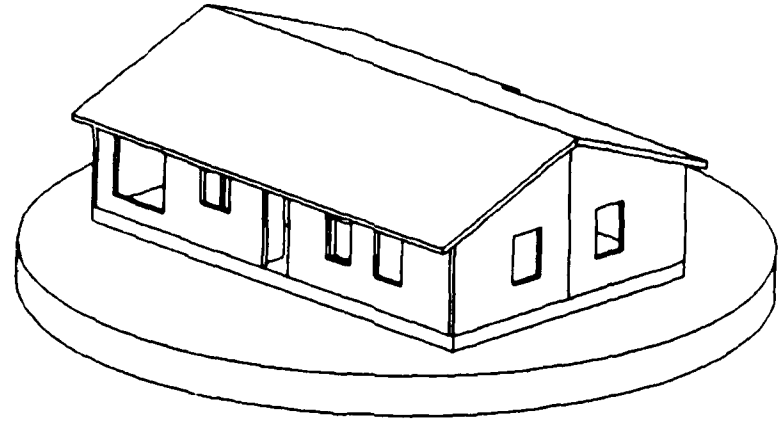

Rear

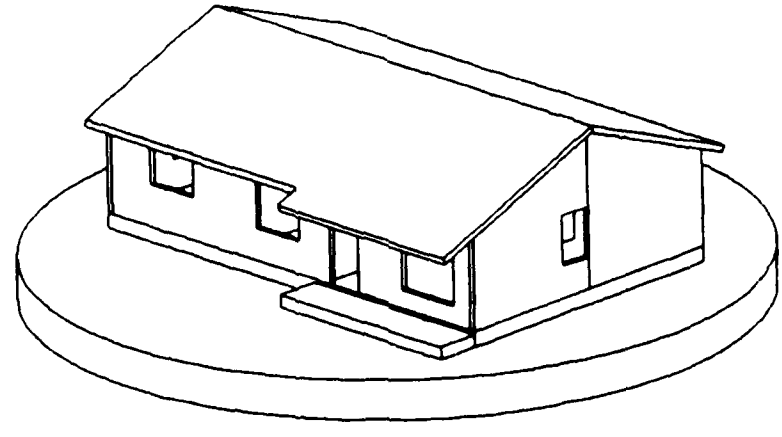

Front

Figure 3. Front and rear views of the wood rambler.

except for an above ground shelter consisting of walls, floor and ceiling of 8 inch thick concrete in the bathroom.

Fallout protection factor experiments were performed on this structure in the late 1950's. In separate parts of the experiment, sources were placed on the roof and on the ground, the latter in the form of a 25.5 ft radius ring about the center of the house. Results of the experiment, reported in Ref. 18 and as used here, were based on a normalization of 1 millicurie per square foot of horizontal roof area and on 2 millicuries per foot of ring circumference.

Dose rates were calculated for five locations along a traverse of the wood rambler centerline. The calculated results are compared with measured results in Fig. 4, which also shows the detector locations on a floor plan drawn by a graphics code from the Monte Carlo geometry. As shown, agreement is generally good, with most dose rates comparing within 10 percent but with two points differing by about 25 percent.

4.7 NTS TWO-STORY BRICK HOUSE.

The NTS two-story brick house was also built at the Nevada Test Site for the 1953 test series. This structure was 33 ft 4 inches in length by 24 ft 8 inches width and had a 79.5 inch deep basement with seven basement windows and an external entry. Front and rear views of the house are given in Figure 5.

The walls of the house were load bearing, comprised of a 4 inches thick brick veneer over 4 inches thick (but hollow) cinderblocks. Reference 18 indicated that the outside wall thickness was "estimated to be 57 lb/ft^2", but on-site measurements of the actual wall dimensions and subsequent measurements of the densities of material samples taken from the wall indicated an actual wall thickness of about 78.6 lb/ft^2.

	Ring Source			Roof Source		
Detector	Experiment	Calculated	Ratio	Experiment	Calculated	Ratio
A	7.73	5.83	0.75	38.0	36.9	0.97
B	4.41	3.65	0.83	43.1	38.8	0.90
C	1.41	1.73	1.23	42.3	48.1	1.14
D	2.00	2.12	1.06	50.0	46.0	0.93
E	6.43	5.96	0.93	52.7	51.2	0.97

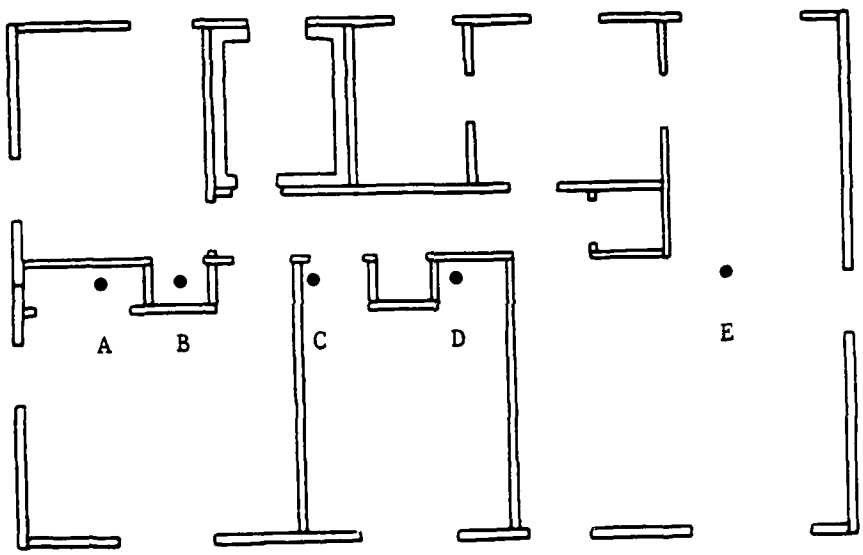

Figure 4. Summary of results for the wood rambler. Values are given in milliroentgens per hour.

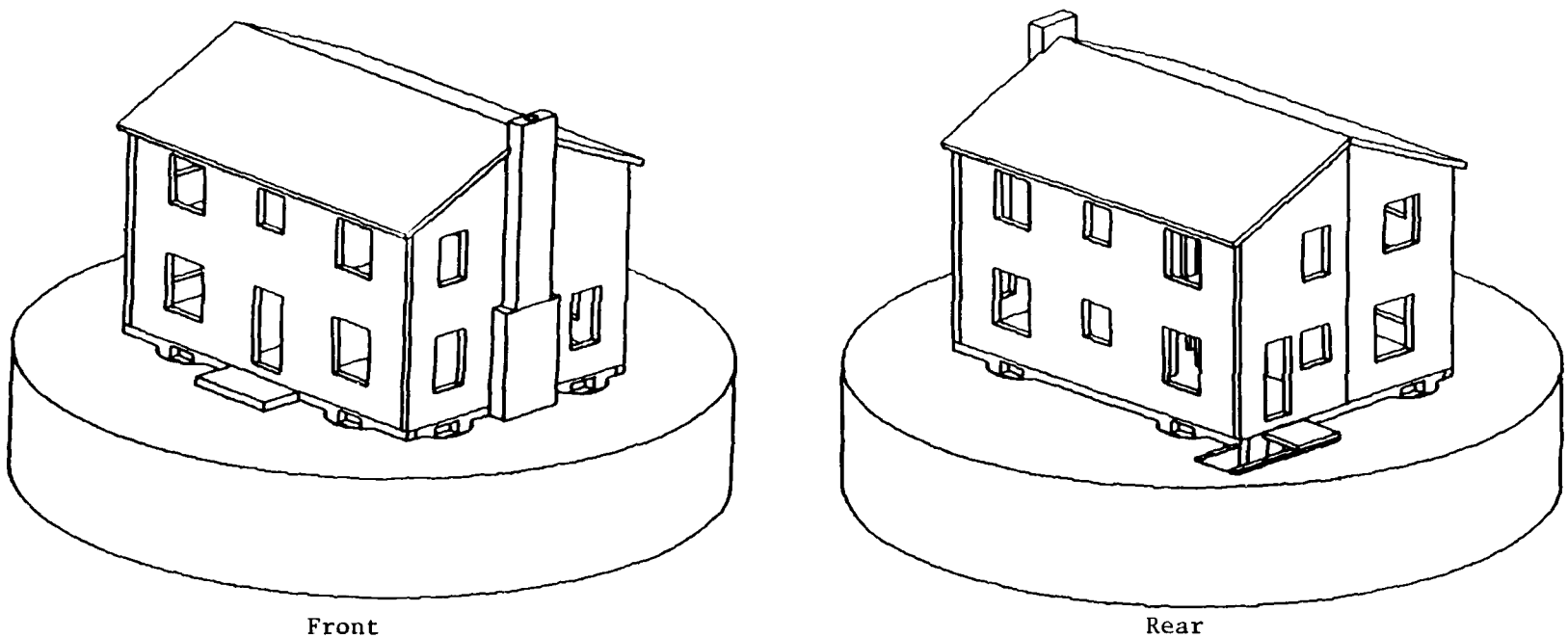

Figure 5. Front and rear views of the NTS two-story brick house.

As with the wood rambler, fallout protection experiments were performed using Cobalt 60 in a ring source configuration on the ground. Unlike the wood rambler, however, no sources were placed on the roof as it had been severely damaged in one of the weapon tests. Instead, measurements were made with two ring sources, one with a radius of 25.5 ft and the other with a radius of 42.5 ft.

Dose rates were calculated for 10 detector locations along corner to corner diagonal traverses. Four detector locations were in the basement and six detector locations were on the first floor. The calculated results for the brick house are compared with measured dose rates in Figure 6. Most results agree within 10 to 15 percent, but three detectors, F, G and J, had calculated dose rates which were nearly a factor of two above the measured dose rates. Further investigation indicated that the dose rates at these positions were very sensitive to detector height because of window sills between the detector and source rings. Reference 18 indicates that the detectors were often 2 to 6 inches below the reported height because of sag in the strings supporting the detectors. Calculations performed with detector locations lowered by 6 inches for these three detectors are in much better agreement with the measured values.

4.8 LONG ISLAND BARRACKS.

The Long Island Barracks was a heavy brick structure located at Fort Strong on Long Island in Boston Harbor. Built around 1910, it was 140 ft 4 inches long by 97 ft 1 inch wide overall, shaped like a large letter U with the long dimension across the bottom of the U. The building, shown in Figure 7, was three floors in height, had a slate roof and no basement (Ref. 23). Unfortunately, the structure was destroyed in the early 1960's, shortly after the radiation transmission experiments were performed.

		25.5 ft Ring Source			42.5 ft Ring Source		
Detector	Floor	Experiment	Calculated	Ratio	Experiment	Calculated	Ratio
A	Bsmt	0.088	0.092	1.05	0.05	0.055	1.10
B	Bsmt	0.167	0.163	0.98	0.08	0.076	0.95
C	Bsmt	0.257	0.218	0.85	0.109	0.150	1.37
D	Bsmt	0.228	0.209	0.92	0.129	0.150	1.16
E	1	2.79	2.39	0.86	1.10	0.98	0.89
F	1	1.60	3.08	1.92	1.39	1.91	1.38
G	1	1.60	1.39	0.88	0.79	1.67	2.11
H	1	1.00	1.11	1.11	0.66	0.80	1.21
I	1	1.02	0.99	0.97	0.79	0.82	1.03
J	1	1.66	3.00	1.80	1.63	1.85	1.13
F*	1	1.60	1.68	1.05	1.39	1.81	1.30
G*	1	1.60	1.23	0.77	0.79	0.96	1.22
J*	1	1.66	1.45	0.87	1.63	1.97	1.21

*Detector lowered by 6 inches for expected string sag.

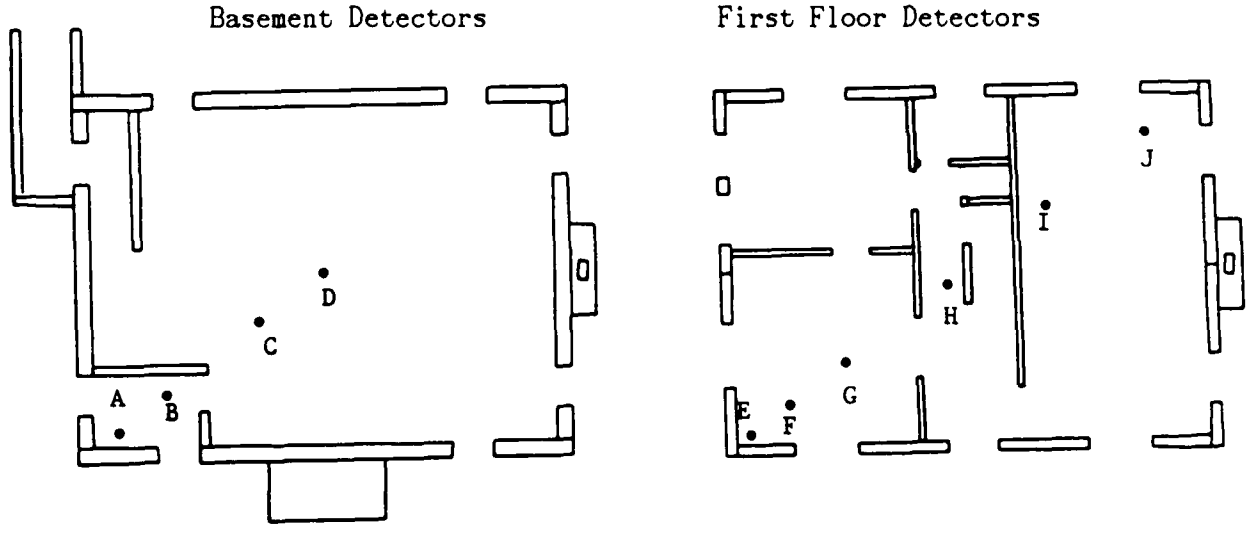

Figure 6. Comparison of calculated and measured results for the two-story brick house. Values are in milliroentgens per hour.

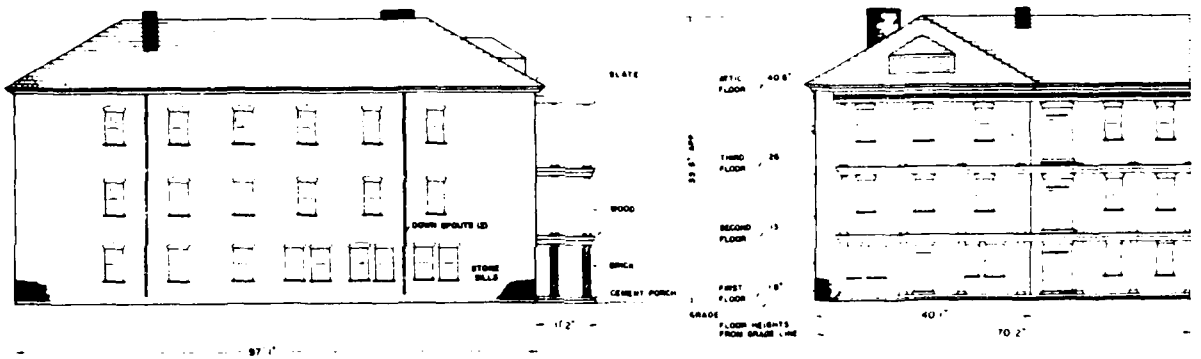

Figure 7. Left side and front elevation views of the Long Island Barracks.

Reference 23 gave a fairly complete description of the barracks, indicating structure dimensions, and floor elevations as well as floor and ceiling thicknesses. The authors of Reference 22, however, were not able to directly determine exterior and interior wall thicknesses and had to infer these from broad beam attenuation of Cobalt 60 radiation through the walls. Their estimates of wall thicknesses were 105 lb/ft^2 for the exterior walls, 125 lb/ft^2 for interior load bearing walls and 4.8 lb/ft^2 for internal partitions.

Simulated fallout dose rate measurements were made using cobalt and iridium sources in annular bands around the building. Four source zones were used, as shown in Figure 8. The first zone extended from the building exterior walls to a radius of 100 ft from the center of the building. The second, third and fourth zones were concentric, with annulus band widths of 25 feet each. Building symmetry was used, reducing the source layout by a factor of two for the inner three zones and by a factor of four for the outer zone.

An area radiation source for each zone was simulated by use of a hydraulic system which consisted of over a kilometer of polyethylene tubing laid out in a pattern in the source zones. The ends of the tube were connected to a large shielded cask which contained an encapsulated radioactive source, either 200 curies of cobalt-60 or from 200 to 400 curies of iridium-192, attached to a small piston designed to fit the polyethylene tubing. A constant volume pump, when actuated, caused the source to emerge from its container and circulate through the tubing, finally returning to its shield at the end of the run.

The initial dose rates calculated with VCS generally differed by about a factor of two from the measured dose rates. Suspecting that the problem was caused by an incorrect or incomplete description of the strucure, a signifiant effort was made to obtain better data. At first telephone calls were made in an attempt to locate as-built drawings or a similar structure at another location. Calls were made to the city of

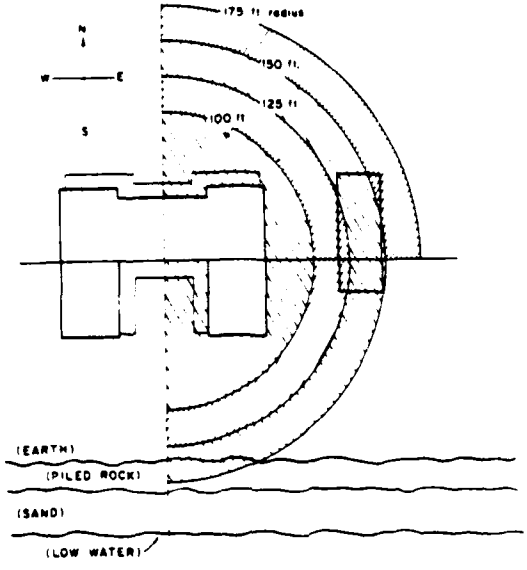

Figure 8. Source distribution around Long Island Barracks.

Boston, the Long Island Hospital (which controls the site), the U.S. Army Engineers, the National Archives in Waltham (just outside Boston), and others. When no additional information was found, a site visit was made to determine what information, if any, could be gleaned from the remains of the structure. Also, in the same trip, a search was made at the National Archives and at the Long Island Hospital for useful material.

The only useful information found on this trip was the correct thickness of the barracks exterior walls. Fortunately, a portion of one of the exterior walls still stood. Unfortunately no interior load bearing walls, floors or partitions, remained in recognizable form. The exterior wall was found to be 12 inches thick (three courses) brick, which, with the density of brick and mortar samples taken, gave an total wall thickness of 126 lb/ft^2 i.e., approximately 20 lb/ft^2 greater than indicated in the literature.

Dose rates were calculated for one detector location on each of the three floors of the Long Island Barracks. The results, given in terms of the dose rate from each of the four source rings, are compared with the measured dose rates in Figure 9. The agreement was substantially better than obtained before the site visit; but still only about half of the calculated results were within 25 percent of the measured results.

It is expected that the remaining differences between calculated and measured dose rates are caused by discrepancies remaining in the structure model. Unless better descriptive information on the structure is found, which appears unlikely at this time, it is doubtful that the differences will be resolved.

Detector	Floor	Source Ring	Dose rate, milliroentgens/hr Measured	Calculated	Ratio
3G	1	1	6.4	7.37	1.15
	1	2	1.5	2.34	1.56
	1	3	1.3	1.70	1.31
	1	4	1.0	1.19	1.19
3C	2	1	5.3	12.3	2.31
	2	2	3.0	4.40	1.47
	2	3	1.5	1.86	1.24
	2	4	1.6	1.63	1.02
8C	3	1	3.4	10.8	3.19
	3	2	1.7	1.83	1.08
	3	3	0.7	0.70	1.01
	3	4	0.5	0.81	1.62

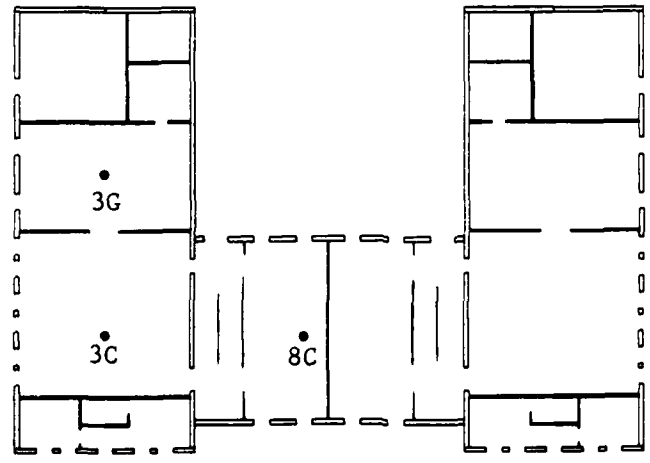

Figure 9. Comparison of measured and calculated Dose Rates for the Long Island Barracks.

SECTION 5
FPF VARIATIONS IN A STRUCTURE CATEGORY

5.1 FPF VARIATIONS IN A SINGLE-STORY WOOD FRAME HOUSE.

5.1.1 Description of the Baseline Structure.

The first structure analyzed for fallout protection factor variations is a single-story wood frame house with a basement. The baseline house is 40 ft in length by 24 ft wide, and has a 20 inch high foundation and side wall heights of 10 ft 6 inches with a peak height of 14 ft 4 inches. The house has a full basement, with the elevation of the basement floor being 65 inches below the ground level.

The house is of standard wood frame construction. The exterior walls are comprised of 2x4 studding 16 inches between centers with three-quarter inch wood sheeting and a half inch of wood siding on the outside and a half inch of drywall plaster board on the inside. The interior walls (partitions) have a similar 2 x4 studding composition, 16 inches between centers, but have half inch drywall plaster board on both sides. The roof is of 2x6 rafters with 16 inch spacing and 3/4 inch plywood sheeting covered by a 3/16 inch thick layer of asphalt shingle. The floor is of 2x10 construction, 12 inches between centers, with 3/4 inch plywood and carpet. The ceiling is of 2x6 construction on 16 inch spacing with a half inch thick drywall plaster board. The foundation thickness is 10 inches of poured concrete.

Figure 10 shows front and rear views of the baseline single story wood frame structure as modeled. Also shown is a plan view of the first floor interior. This plan view shows the "detector" locations where the protection factors are evaluated. Locations A, B, C and D are in the basement, and locations E, F, G and H are on the first floor. All protection factors were evaluated at a point 3 ft above the floor level.

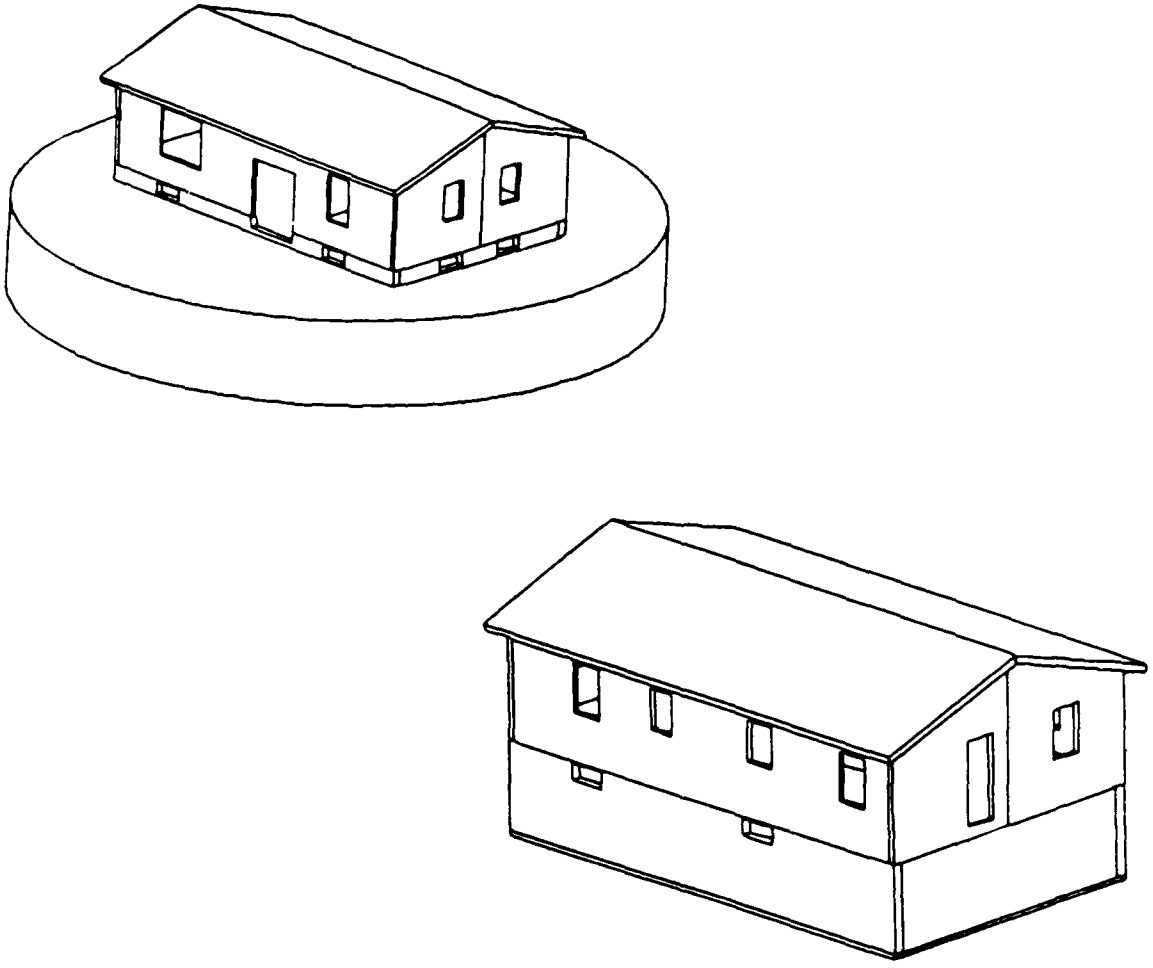

Figure 10. Single-story wood frame house with basement.

5.1.2 Analysis of the Baseline Single-Story Wood Frame Structure.

The protection factors calculated for the baseline single-story wood frame structure basement and first floor are as follows:

Table 5. Protection factor results for the baseline single-story wood frame structure.

Basement		First Floor	
Point A	8.48	Point E	1.45
B	7.32	F	1.56
C	8.02	G	1.67
D	10.97	H	1.52

The above results show the expected large difference between basement and first floor protection factors. The basement protection factors are largest for locations near the walls or corners where the basement walls reduce the view solid angle of the floor area above, from which nearly all of the radiation dose to basement locations comes. The protection factors for the first floor see the opposite effect, i.e., the protection factors are highest at the center of the structure and lowest near the walls. This difference between the basement and first floor protection factor profiles is caused by the relative importance of the radiation transmitted through the walls and the radiation coming from above. The shielding effect of the basement walls is large, while the shielding effect of the first floor walls is small.

5.1.3 Analysis of Structure Variations.

Calculations were performed to determine the effect of different basement depths, of having no basement, of having an attached garage, and of having no internal partitions (walls). The results of these calculations are described below.

Two additional calculations were performed to explore the effect of different basement depths. The protection factors, evaluated for location A in the basement, were as follows (the result for the baseline case has also been included below to facilitate comparison):

Table 6. Variations of single-story wood frame protection factors with basement depth.

50 inch deep basement, location A	7.09
65 inch deep basement (baseline)	8.48
80 inch deep basement	9.39

The variation with basement depth is clear for basements ranging from shallow to deep. The protection factor increases with basement depth, as expected, with an increase of about 33 percent seen for a deep basement as compared to a shallow basement.

The effect of a basement on the first floor protection factors was explored by altering the structure to eliminate the basement. Two calculations were performed on the structure with no basement; for the first calculation the basement window penetrations through the foundation were assumed to still exist, while for the second calculation the basement windows were eliminated. The results, calculated for detector location G and compared with the results of the baseline structure (with basement) are compared below:

Table 7. Effect of a basement on single-story wood frame house first floor protection factors.

Baseline house (with basement)	1.67
Basement removed, but with foundation penetrations	1.65
Basement and foundation penetrations removed	1.67

The above results indicate that the effect of a basement on above-ground protection factors is small. Also, the effect of basement windows on above-ground protection factors is small. The difference between the above results (1.67 and 1.65) is within the Monte Carlo

statistics and are not believed to be meaningful, although it is expected that foundation penetrations would usually slightly decrease the above-ground protection factors.

The third variation investigated was the effect of an attached garage. Figure 11 shows the modified structure with the added garage. Protection factors were calculated in one basement location (location B) and one first-floor location (location G). These results, compared with the baseline, are as follows:

Table 8. Effect of an attached garage on the single-story wood frame house protection factors.

Location B without garage (baseline)	7.32
Location B with garage	7.01
Location G without garage (baseline)	1.67
Location G with garage	1.69

These results indicate that an attached garage can be expected to slightly reduce the protection factor in the basement. The decrease in the basement protection factor is caused by the relocation of part of the fallout radiation source from the ground under the garage roof (where the source is shielded by the basement wall and foundation) to the roof, where the line-of-sight shielding is considerably reduced. The difference between the with- and without-garage results for the first floor are within Monte Carlo statistics and are not meaningful.

The last variation on the single-story wood frame house was the effect of the internal partions. To explore the effects of the internal partitions, a calculation was performed on the structure with all the internal partitions removed. The results, calculated for location G, are compared with the results for the baseline structure below.

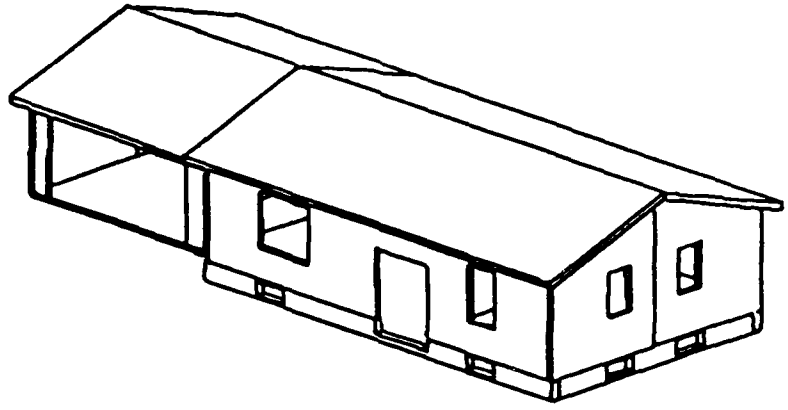

Front

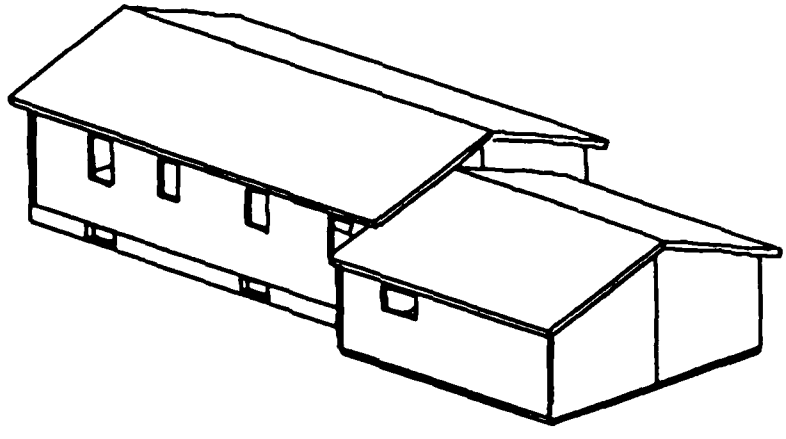

Rear

Figure 11. Single-story wood frame house with attached garage.

Table 9. Effect of internal partitions on single-story wood frame house protection factors.

Location G with partitions (baseline)	1.67
Location G without partitions	1.42

The above results indicate that the internal partitions can significantly affect the protection factor for a light structure. This is not in agreement with observations by Robinson, et. al, (Reference 21). However in the structure analyzed by Robinson, the partitions did not obscure the line of sight toward all walls as is the case here for location G. Also, the structure treated by Robinson had thicker exterior walls.

5.2 FPF VARIATIONS IN A TWO-STORY BRICK FACE HOUSE.

5.2.1 Description of the Baseline Structure.

The second structure analyzed for fallout protection factor variations is a two-story brick face house with a basement. The baseline house is nearly square, being 32 ft long by 28 ft wide. It has a 30 inch high foundation, side wall heights of 20 ft 1 inch, and a peak height of 30 ft. The house has a full basement with the elevation of the basement floor being 54 inches below the ground level.

The house is of standard wood frame brick face construction. The exterior walls are comprised of 2x4 studding 16 inches between centers with a four-inch thick layer of brick and mortar on the outside and and a half inch of drywall plaster board on the inside. The interior walls (partitions) are the same as for the single-story wood frame house, i.e., 2 x4 studding 16 inches between centers with a half inch drywall plaster board on both sides. The roof is of 2x6 rafters with 16 inch spacing and 3/4 inch plywood sheeting covered by a half inch thick layer of wood shingles. The floor is of 2x10 joists, 16 inches between centers, with 3/4 inch plywood. The first-floor ceiling is of 2x8 construction on 16 inch

spacing with 3/4 inch plywood above and half inch thick drywall plaster board below. The second-floor ceiling is 2x6 construction on 16 inch spacing with a half inch thick drywall plasterboard below. The foundation thickness is 10 inches of poured concrete.

Figure 12 shows front and rear views of the baseline two-story brick face structure as modeled, and figure 13 shows plan views of the first and second floor interiors. The plan views also show locations where the protection factors were evaluated. Locations A and B are in the basement, locations C and D are on the first floor, and locations E and F are on the second floor. All protection factors were evaluated at a point 3 ft above the floor level.

5.2.2 Analysis of the Baseline Two-Story Brick Face Structure.

The protection factors calculated for the baseline two-story brick face structure are as follows:

Table 10. Protection factor results for the baseline two-story brick face structure.

Location A, Basement center	13.9
Location B, Basement quadrant	15.3
Location C, First floor center	3.57
Location D, First floor quadrant	3.20
Location E, Second floor near center	3.51
Location F, Second floor quadrant	3.40

As with the single-story wood frame house, the above results show a large difference between basement and above-ground protection factors. The basement protection factors are largest for locations near the walls or corners where the basement walls reduce the view solid angle of the floor area above. The above-ground protection factors see the opposite effect, i.e., the protection factors are highest at the center of the structure and lowest near the walls. There is very little difference between the first-floor protection factors and the second-floor protection factors for this structure.

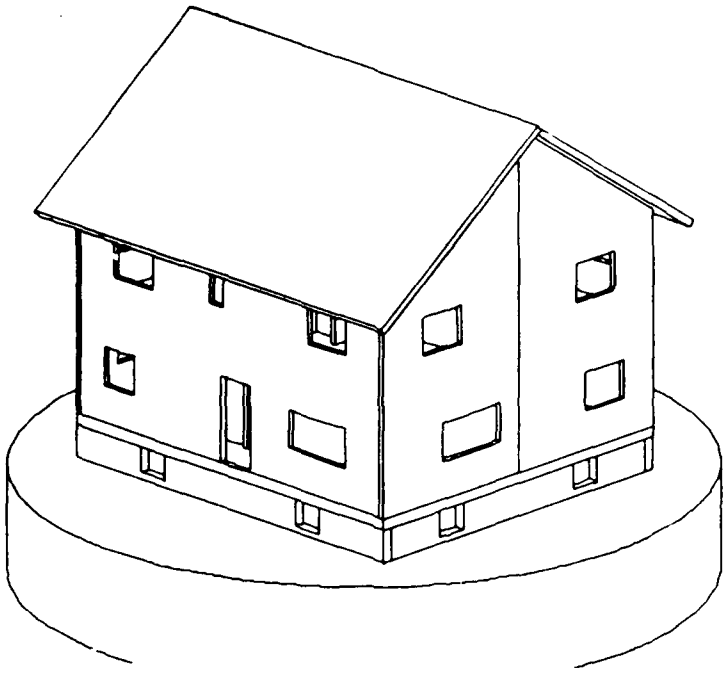

Front

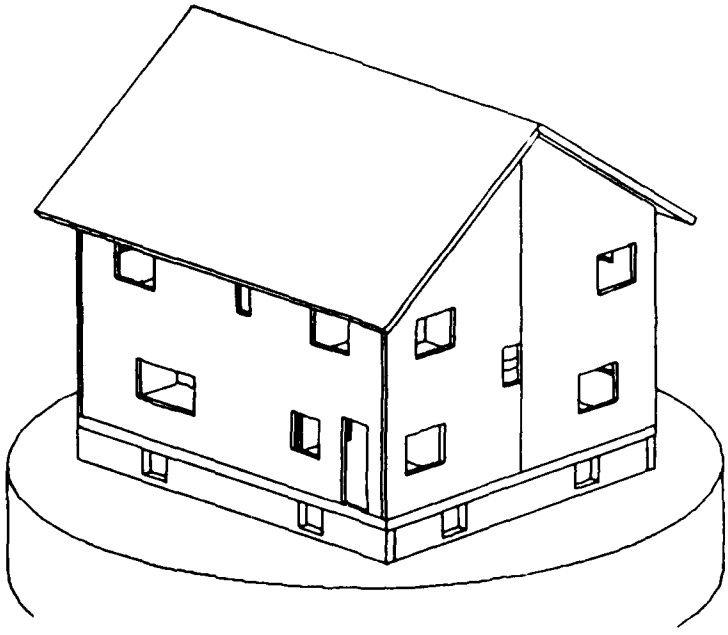

Rear

Figure 12. Baseline two-story brick faced house.

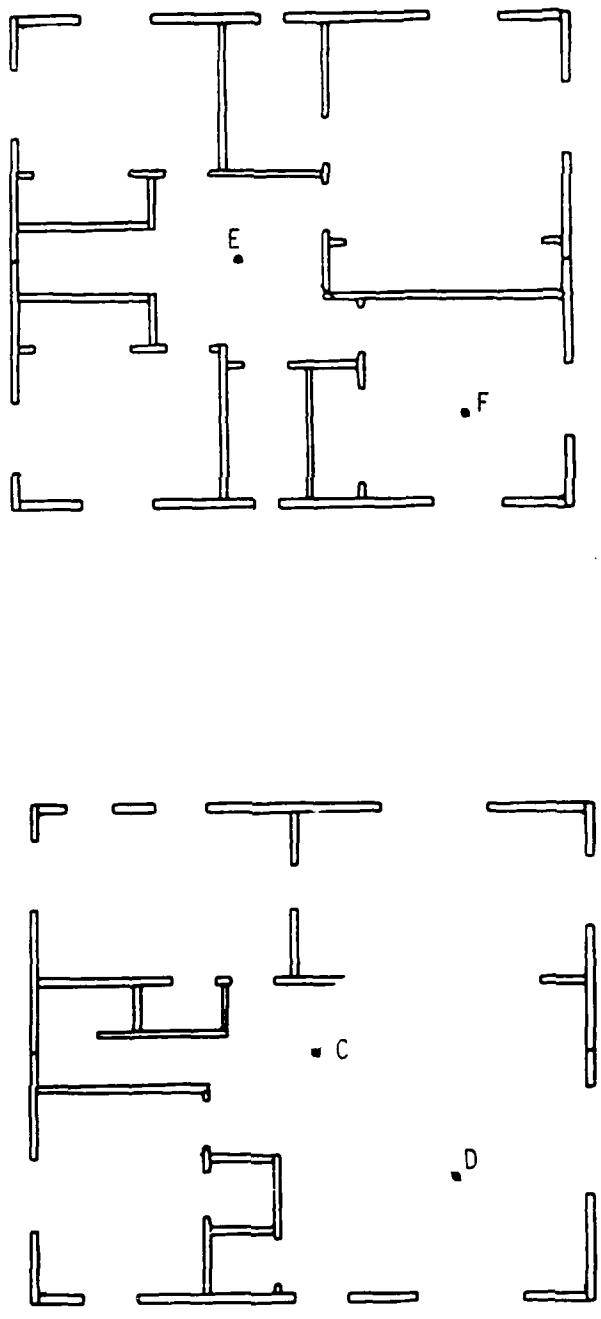

Figure 13. Interior of two-story brick faced house.

5.2.3 Analysis of Structure Variations.

Calculations were performed to determine the effect of a different length-to-width ratio for the house, of different window sizes, and of having fewer or no internal partitions. The results of these calculations are described below.

A calculation was performed with the house length and width modified to 37 ft 4 inches and 24 ft, respectively (Figure 14). These new dimensions preserved the total floor area of the structure. The protection factor, evaluated for location C (on the first floor), is as follows (the result for the baseline case has also been included to facilitate comparison):

Table 11. Variation in two-story brick face protection factors with structure length-to-width ratio.

32 ft by 28 ft house (baseline)	3.57
37 ft 4 in by 24 ft house	3.62

The differences between the results are within Monte Carlo statistics and are not significant.

The effect of window sizes on the first floor protection factor was explored by altering the structure to exactly double the area of the the first and second floor windows (Figure 15). The protection factor result for detector location C is compared with the corresponding result for the baseline structure below:

Table 12. Effect of window size on two-story brick face house first floor protection factor.

Baseline house	3.57
House with enlarged windows	2.73

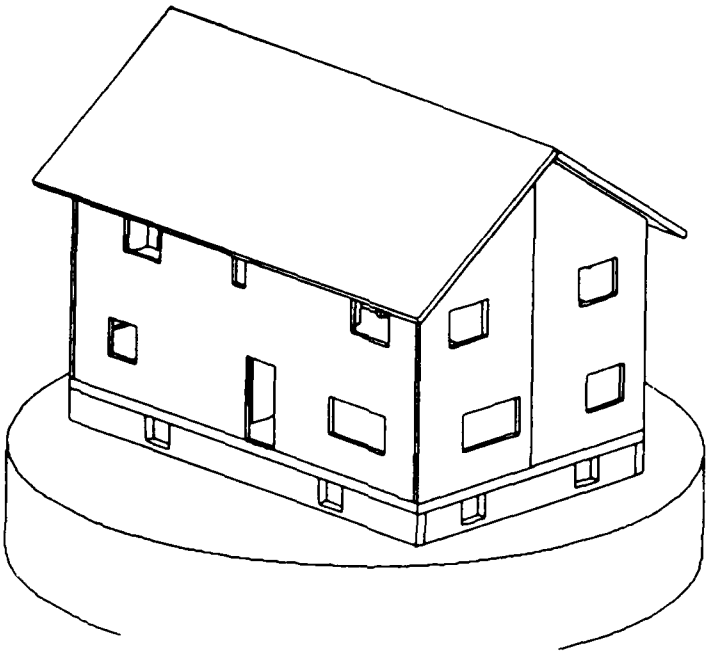

Front

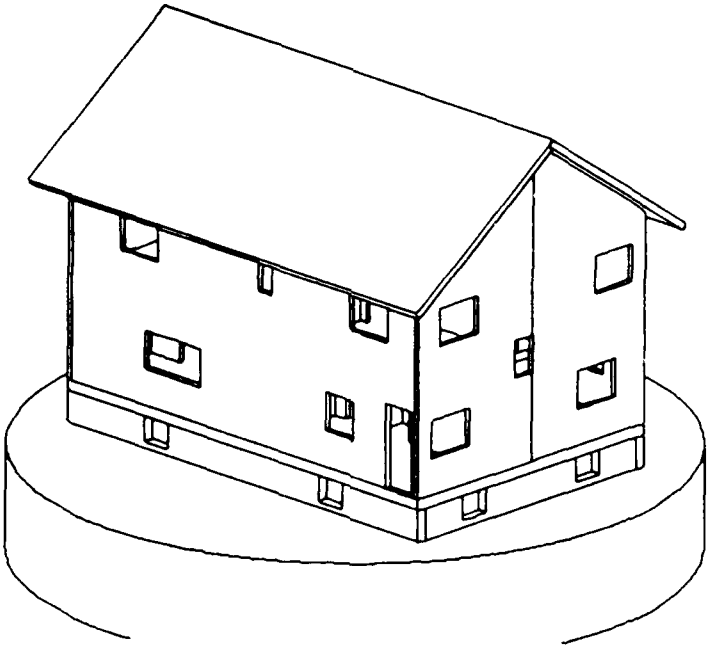

Rear

Figure 14. Elongated two-story brick house.

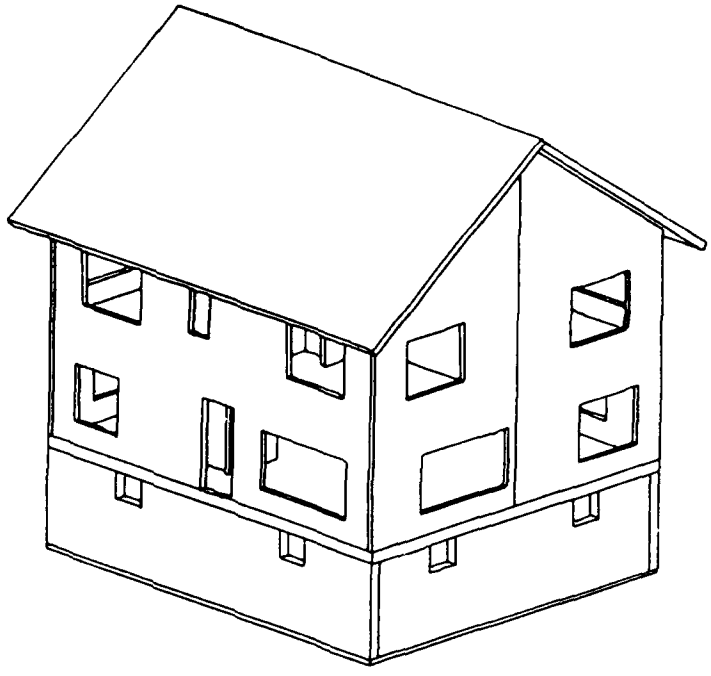

Front

Soil is transparent
in this figure

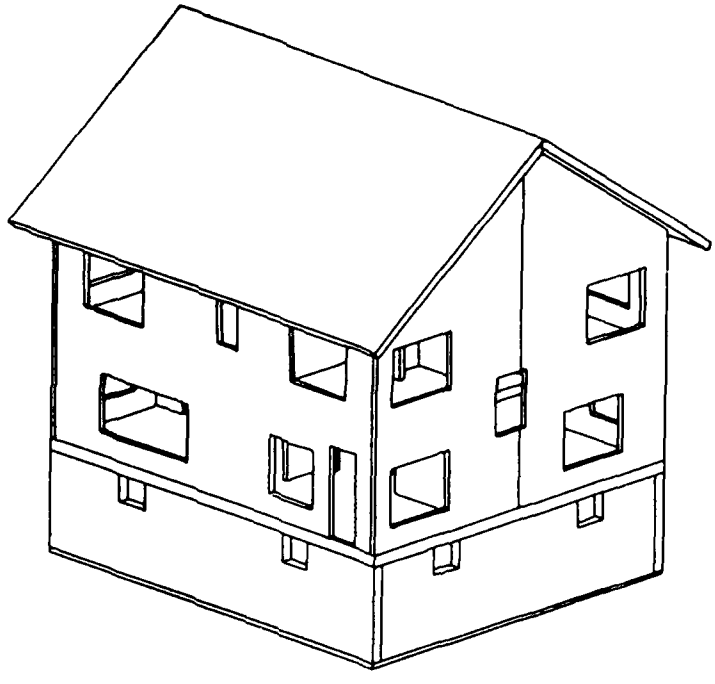

Rear

Figure 15. Two-story brick house with enlarged windows.

The above results indicate that the effect of window size on above-ground protection factors of the two-story brick face house is significant. These data indicate that window size can affect the protection factors for this type of structure by up to 30 percent.

The last variation investigated for the two-story brick face house was the effect of the internal partitions. To explore the effects of the internal partitions, a calculation was performed on the structure with all the internal partitions removed. The result, calculated for location C, is compared with the result for the baseline structure below.

Table 13. Effect of internal partitions on two-story brick face protection factors.

Location C with partitions (baseline)	3.57
Location C without partitions	3.30

The above results indicate that the internal partitions have a small effect on the protection factor for the brick structure. This conclusion differs from that made for the single story wood frame house; however, the mass thickness of the partitions, while the same for both structures, contributes a smaller fraction of the total shielding effect to the two story brick face structure than to the single-story wood frame structure.

5.3 FPF VARIATIONS IN A THREE-TO FIVE-STORY BRICK FACE APARTMENT BUILDING.

5.3.1 Description of the Baseline Structure.

The third structure analyzed for fallout protection factor variations is a four-story brick face apartment house with a basement. The baseline structure is 133 ft 4 inches long by 66 ft 8 inches wide. It is 35 ft 10 inches high, has a flat roof (Figure 16), and has a full basement with the elevation of the basement floor being 90 inches below the ground level. It has a 6-inch high foundation.

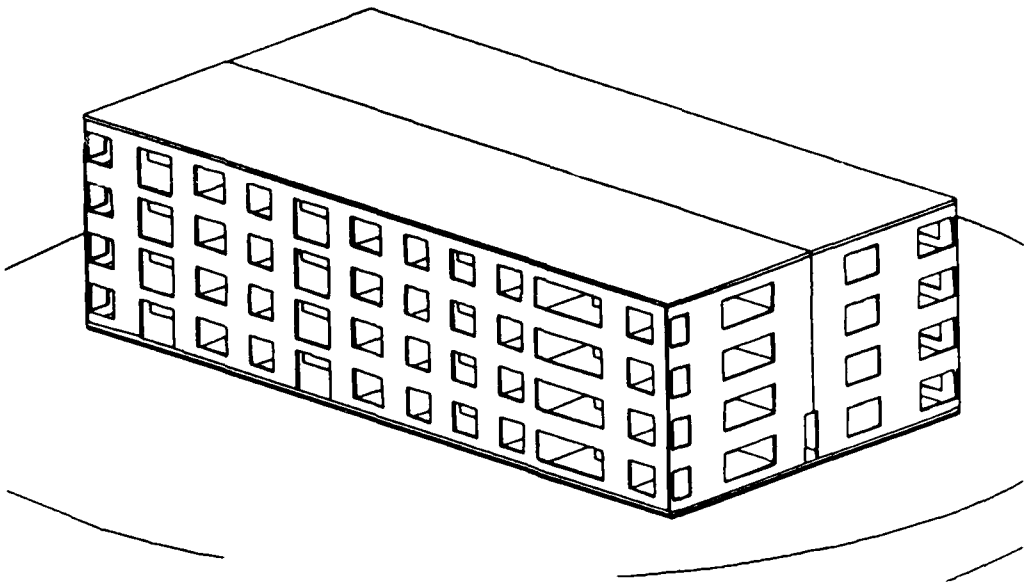

Right side and rear

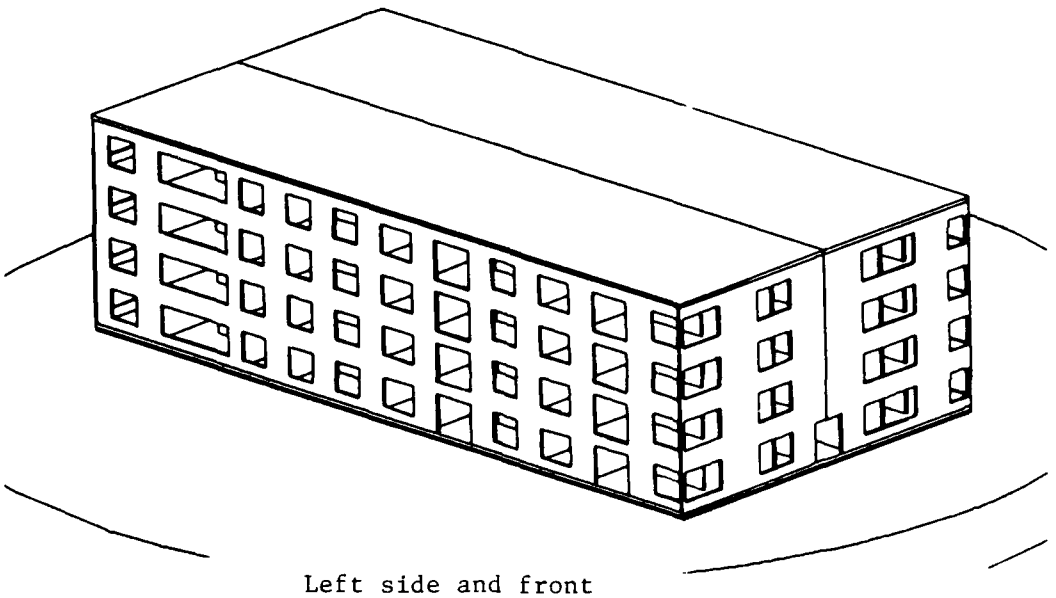

Left side and front

Figure 16. Four-story apartment building.

The exterior walls of the structure are comprised of 2x4 studding 16 inches between centers with a four inch thick layer of brick and mortar and 3/4 inch plywood sheeting on the outside and and a half inch of drywall plaster board on the inside. The interior walls (partitions) are the same as for the single-story wood frame house, i.e., 2 x4 studding 16 inches between centers with a half inch drywall plaster board on both sides. The first floor is of 8 inch thick concrete. The upper-level floors and the roof are of 8 inch thick 50 percent density concrete, with a half inch of drywall plasterboard on the underside of the ceilings and a quarter inch of asphalt roofing on the roof. The foundation thickness is 10 inches of poured concrete.

Figure 17 shows the floorplan, with all floors being the same. The floorplan shows three of the four locations where protection factors were evaluated. Location A is at the center of a basement quadrant and is not shown; locations B, C and D apply to each floor. All protection factors were evaluated at a point 3 ft above the floor level.

5.3.2 Analysis of the Baseline Four-Story Brick Face Structure.

The protection factors calculated for the baseline four-story brick face structure are as follows:

Table 14. Protection factor results for the baseline four-story brick face structure.

Location A, Basement quadrant	531.
Location B, First floor	9.18
Location B, Second floor	17.2
Location B, Third floor	18.0
Location C, Third floor	17.3
Location D, Third floor	13.9
Location B, Fourth floor	10.9

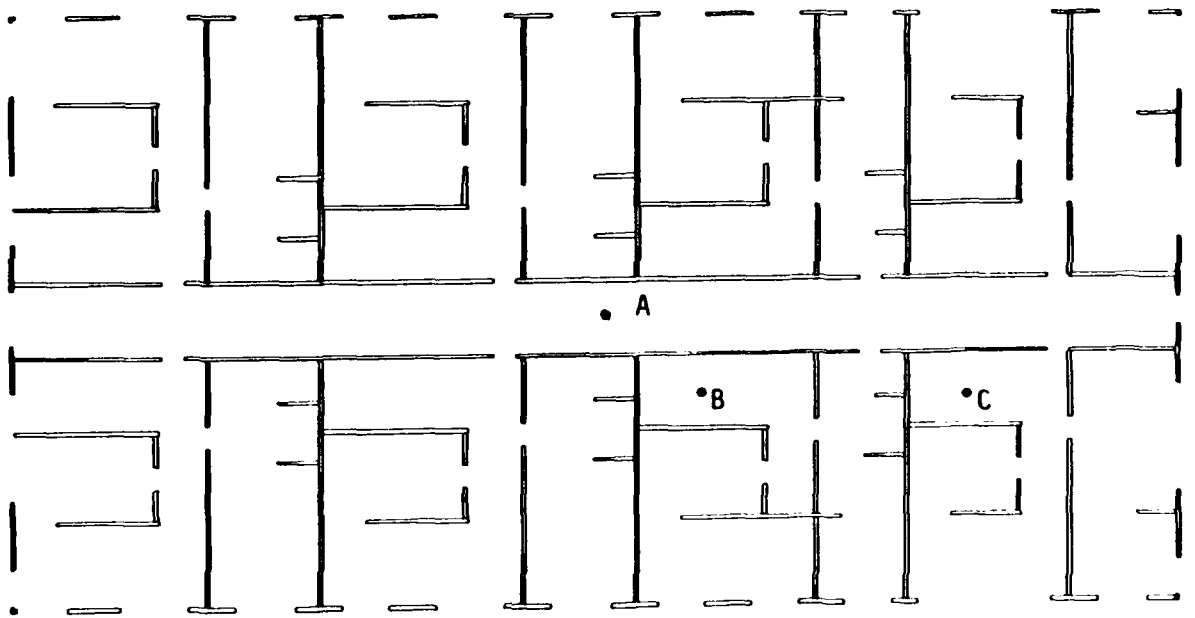

Figure 17. Floor plan of apartment building showing protection factor locations.

As with the single-story wood frame and two-story brick face houses, the above results show a large difference between basement and above-ground protection factors. The protection factors for the second and third floors are larger than those for the first and fourth floors. This is because the second and third floors are farther from the fallout radiation sources on the ground and roof and because the intermediate floors provide additional shielding between the fallout radiation source and the "detector" location.

5.3.3 Analysis of Structure Variations.

Calculations were performed to explore the effect of different numbers of floors in the structure, of balconies on upper-level floors, and of having fewer or no internal partitions. The results of these calculations are described below.

Calculations of the protection factor in the basement quadrant (point A) and the center of the first floor (point B) were performed for three- and five-story apartment buildings which differed from the baseline four-story structure only by the addition or deletion of one intermediate floor. The structures analyzed are shown in figure 18. The protection factors, evaluated for locations A and B, are as follows (the result for the baseline case has also been included to facilitate comparison):

Table 15. Variation in apartment house protection factors with the number of floors.

Three-story structure, point A (basement)	457
Four-story structure, point A (basement)	531
Five-story structure, point A (basement)	572
Three-story structure, point B (first floor)	8.6
Four story structure, point B (first floor)	9.2
Five story structure, point B (first floor)	9.9

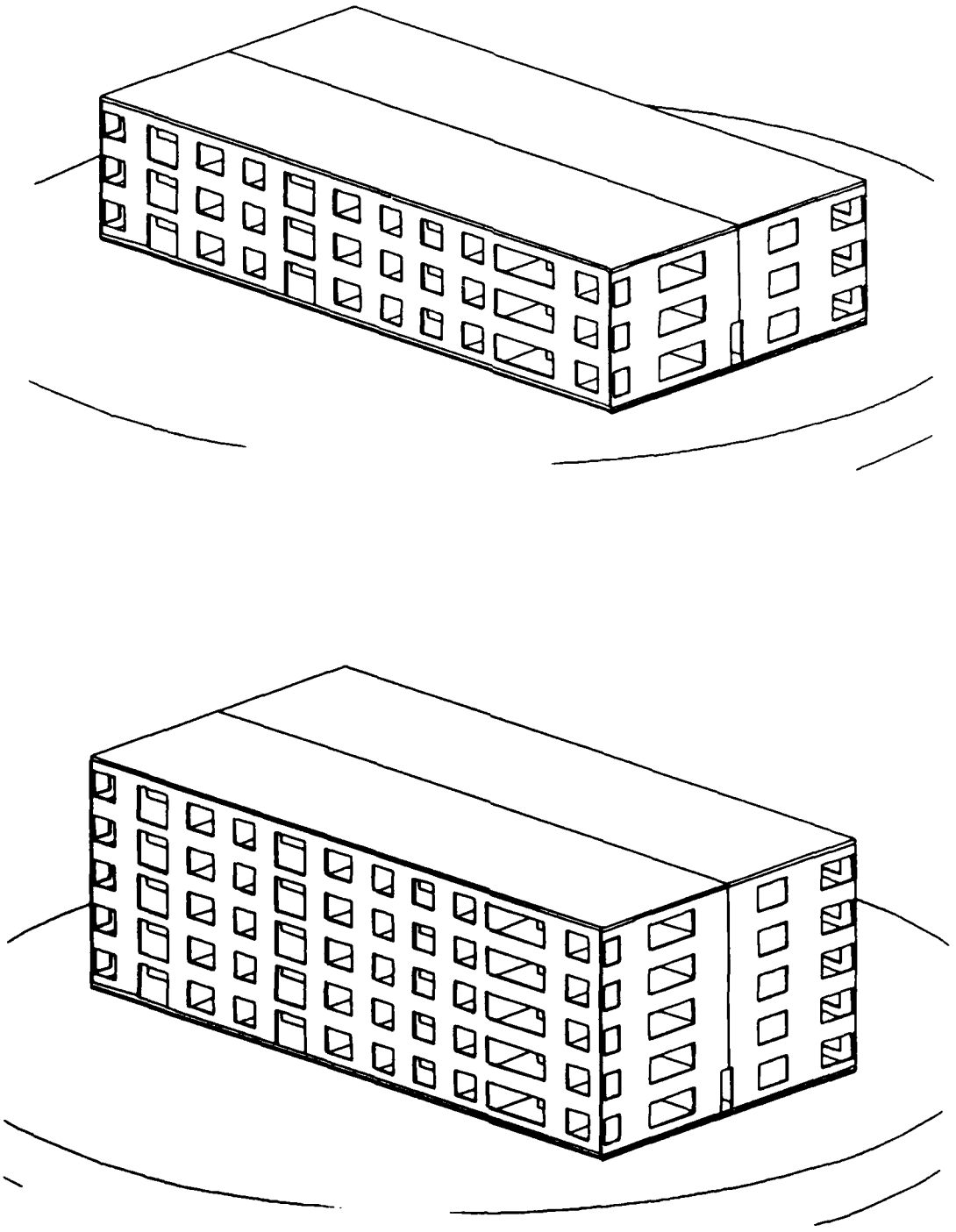

Figure 18. Three and five-story apartment structure variations.

The effect of balconies on the protection factor was explored by altering the structure to include an external balcony for each apartment as shown in figure 19. The balconies were assumed to be of the same materials and thickness as the floors, i.e., 8 inch thick 50 percent density concrete, or of wood (2 by 6 joists with 16 inch spacing supporting 3/4 inch thick flooring). The balconies were assumed to be contaminated with fallout to the same density as the fallout on the surrounding soil surfaces. The protection factor results for detector location B on the third floor are compared with the corresponding result for the baseline structure below:

Table 16. Effect of balconies on four-story apartment house third floor protection factor.

Baseline structure	18.0
Structure with concrete balconies	18.5
Structure with wood balconies	18.0

The above results indicate that balconies do not greatly affect the protection factors for the particular situation, i.e., an intermediate level floor on a brick faced apartment building for a "detector" location fairly deep within the structure. It may be expected that "detector" locations nearer the balconies would show a much larger effect, but no calculations were performed for such locations.

The last variation investigated for the four-story brick face apartment house was the effect of the internal partitions. To explore the effects of the internal partitions, a calculation was performed on the structure with all the internal partitions removed. The result, calculated for location B on the first floor, is compared with the result for the baseline structure below.

Table 17. Effect of internal partitions on four-story brick face apartment building protection factors.

Location B with partitions (baseline)	9.2
Location B without partitions	4.9

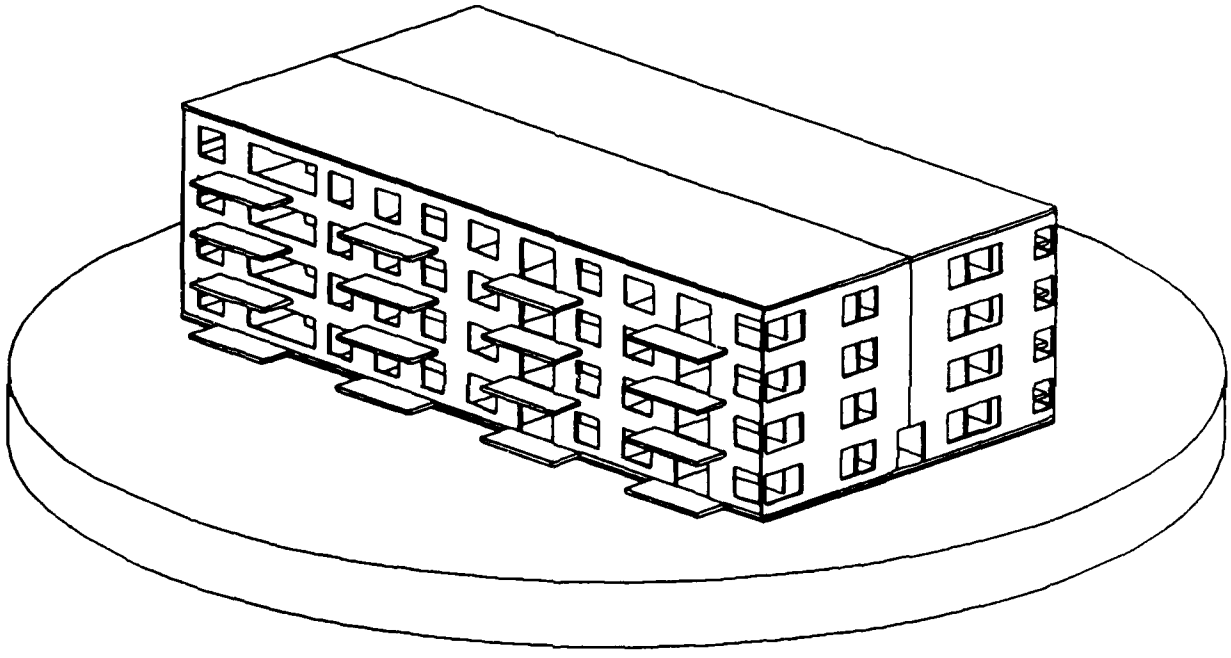

Figure 19. Four-story apartment building with balconies.

The above results indicate that the internal partitions have a significant effect on the protection factor for the brick faced apartment building. This conclusion differs from that made for the two-story brick faced house. However, the apartment building has many more partitions than the two-story brick faced house, so that the total shielding effect of the partitions is greater for the apartment building than for the house. Also, the window sizes on the apartment structure are large, reducing the relative importance of the shielding in the outer walls.

SECTION 6

LIST OF REFERENCES

1. "Structure Shielding Against Fallout Radiation from Nuclear Weapons," National Bureau of Standards, NBS Monograph 42 (1 June 1982).

2. L.V. Spencer, et al., "Structure Shielding Against Fallout Gamma Rays from Nuclear Detonations," National Bureau of Standards, NBS SP 570 September 1980).

3. "PFCOMP, Building Fallout Radiation Protection Factor Analysis," Oak Ridge National Laboratory RSIC Computer Code Collection, CCC-106, no date.

4. "National Facility Survey Instructions," Federal Emergency Management Agency, TR-84 (May 1983).

5. Martin O. Cohen and Mendel Beer, "The Use of Soil as an Expedient Countermeasure for Rural Fallout Shelters," Mathematical Applications Group, Inc., MR-7042, AD/A-006289 (October 1974).

6. W.A. Rhodes, et al., "Vehicle Code System (VCS) User's Manual," Oak Ridge National Laboratory, ORNL-TM-4648 (August 1974).

7. William H. Scott, Jr., "Vehicle Code System (VCS) Documentation and Uncertainty Analysis," Science Applications, Inc., SAI-133-79-977-LJ (December 7, 1979).

8. William A. Woolson, et al., "Coupled House-Man Shielding Calculations for Atomic Bomb Survivor Organ Dosimetry," Second US-Japan Joint Workshop for Reassessment of Atomic Bomb Radiation Dosimetry in Hiroshima and Nagasaki, Hiroshima, Japan (8-9 November 1983).

9. William A. Woolson and Michael L. Gritzner, "Calculation of the BREN Japanese House Shielding Experiments," Science Applications International Corporation, SAI-83-1020 (22 August 1983).

10. M.B. Emmett, "The MORSE Monte Carlo Radiation Transport Code System," Oak Ridge National Laboratory, ORNL-4972 (February 1975).

11. W.A. RHODES and F.R. MYNATT, "The DOTIII Two-Dimensional Discrete Ordinates Transport Code," Oak Ridge National Laboratory, ORNL-4280 (1973).

12. T.J. Hoffman, J.C. Robinson, P.N. Stevens, "The Adjoint Difference Method and its Application to Deep-Penetration Radiation Transport," Nuclear Science and Engineering, 48, pp. 179-188 (1972).

13. George I. Bell and Samuel Glasstone, Nuclear Reactor Theory, Van Nostrand Reinhold Company, New York (1970).

14. "ANISN-ORNL, Multigroup One-Dimensional Discrete Ordinates Transport Code with Anisotropic Scattering," Oak Ridge National Laboratory RSIC Computer Code Collection, CCC-254, no date.

15. "A Capsule Review of the Computer Code Collection (CCC) Peripheral Shielding Routine (PSR) and Data Library Collection (DLC)," Oak Ridge National Laboratory RSIC Memorandum dated January 1982.

16. S.P. Finn, "Calculation of Fission Product Gamma Ray and Beta Spectra at Selected Times After Fast Fission of U-238 and U-235 and Thermal Fission of U-235," Science Applications memo dated 9 November 1979.

17. "DLC-31/(DPL-1/FEWG1), 37 Neutron, 21 Gamma Ray Coupled, P3, Multigroup Library in ANISN Format" Oak Ridge National Laboratory RSIC Data Library Collection (June 1976).

18. C. Eisenhauer, "Analysis of Experiments on Light Residential Structures with Distributed Co-60 Sources," National Bureau of Standards, NBS Report 6539 (15 October 1959).

19. Anthony Foderano, The Photon Shielding Manual, The Penn State Bookstore (July 1976).

20. Murray A. Schmoke and Ralph E. Rexroad, "Attenuation of Fallout Radiation as a Function of Concrete Blockhouse Wall Thickness," Edgewood Arsenal, NDL-TR-43, AD 431063, October 1963.

21. M.J. Robinson, et al., "A University Design Study of Protection Factors in Typical American Houses," Kansas State University Department of Nuclear Engineering, KEES-SR-84 (30 November 1969).

22. J.A. Auxier, et al., "Experimental Evaluation of the Radiation Protection Afforded by Residential Structures Against Distributed Sources," Civil Effects Test Operations, CEX-58.1 (19 January 1959).

23. Eric T. Clarke, et al., "Measurement of Attenuation in Existing Structures of Radiation from Simulated Fallout," Technical Operations Inc., TO-B 59-4 (27 April 1959).

DISTRIBUTION LIST

DEPARTMENT OF DEFENSE

ASSISTANT TO THE SECRETARY OF DEFENSE
ATOMIC ENERGY
ATTN: EXECUTIVE ASSISTANT

DEFENSE INTELLIGENCE AGENCY
2 CYS ATTN: RTS-2B

DEFENSE NUCLEAR AGENCY
ATTN: NANF
ATTN: NASF
ATTN: OPNA
ATTN: RAAE
ATTN: SPWE
4 CYS ATTN: TITL

DEFENSE NUCLEAR AGENCY
ATTN: TDTT W SUMMA

DEFENSE TECHNICAL INFORMATION CENTER
12 CYS ATTN: DD

DNA PACOM LIAISON OFFICE
ATTN: DNALO

FIELD COMMAND DEFENSE NUCLEAR AGENCY
ATTN: FCPR
ATTN: FCTXE

JOINT DATA SYSTEM SUPPORT CTR
ATTN: C-312 R MASON

JOINT STRAT TGT PLANNING STAFF
ATTN: JK (ATTN: DNA REP)
ATTN: JKAD
ATTN: JKCS
ATTN: JLAC
ATTN: JP
ATTN: JPEP

LAWRENCE LIVERMORE NATIONAL LABORATORY
ATTN: DNA-LL

UNDER SECRETARY OF DEFENSE
ATTN: STRAT & SPACE SYS(OS)

DEPARTMENT OF THE ARMY

HARRY DIAMOND LABORATORIES
ATTN: SCHLD-NW-P J BRAND

U S ARMY BALLISTIC RESEARCH LAB
2 CYS ATTN: DRDAR-BLV-R J MALONEY
ATTN: SLCBR-SS-T (TECH LIB)

U S ARMY NUCLEAR & CHEMICAL AGENCY
ATTN: LIBRARY
ATTN: MONA-NU

DEPARTMENT OF THE NAVY

NAVAL AIR SYSTEMS COMMAND
ATTN: AIR-516

NAVAL ELECTRONICS ENGRG ACTVY PAC F C
ATTN: CODE 250 D OBRYHIM

DEPARTMENT OF THE AIR FORCE

AIR FORCE WEAPONS LABORATORY
ATTN: SUL

AIR UNIVERSITY LIBRARY
ATTN: AUL-LSE

AIR WEATHER SERVICE, MAC
ATTN: AWSAE

STRATEGIC AIR COMMAND/DEPR
ATTN: DEPR

STRATEGIC AIR COMMAND/DOTTD
ATTN: DOTU

STRATEGIC AIR COMMAND/DOWE
ATTN: DOWE

STRATEGIC AIR COMMAND/NRI-STINFO
ATTN: NRI/STINFO

DEPARTMENT OF ENERGY

LAWRENCE LIVERMORE NATIONAL LAB
ATTN: L-262 J KNOX
ATTN: L-383 D S MYERS
ATTN: L-53 TECH INFO DEPT LIB

LOS ALAMOS NATIONAL LABORATORY
ATTN: F601 T DOWLER

OAK RIDGE NATIONAL LABORATORY
ATTN: D INGERSOIL
ATTN: G KERR
ATTN: J PACE

SANDIA NATIONAL LABORATORIES
ATTN: TECH LIB 3141/RPTS RCVG CLRK
ATTN: 0332 J W KEIZUR

OTHER GOVERNMENT

CENTRAL INTELLIGENCE AGENCY
ATTN: OSWR/NED
ATTN: SOVA/SIG/SP/D

FEDERAL EMERGENCY MANAGEMENT AGENCY
ATTN: T REID

U S ARMS CONTROL & DISARMAMENT AGCY
ATTN: OPS & ANALYSIS DIV W DEEMER

DEPARTMENT OF DEFENSE CONTRACTORS

ATMOSPHERIC SCIENCE ASSOCIATES
ATTN: H NORMENT

DECISION-SCIENCE APPLICATIONS, INC
ATTN: DR PUGH

KAMAN SCIENCES CORP
ATTN E CONRAD

KAMAN SCIENCES CORPORATION
ATTN DASIAC

KAMAN TEMPO
ATTN: DASIAC

PACIFIC-SIERRA RESEARCH CORP
ATTN: H BRODE, CHAIRMAN SAGE

R & D ASSOCIATES
ATTN: C KNOWLES

RAND CORP
ATTN: P DAVIS

RAND CORP
ATTN: B BENNETT

SCIENCE APPLICATIONS INTL CORP
ATTN: D HAMLIN
ATTN: E SWICK
2 CYS ATTN: J STODDARD
ATTN: M K DRAKE
ATTN: W SCOTT
ATTN: W WOOLSON

SCIENCE APPLICATIONS INTL CORP
ATTN: J MCGAHAN